Cerebral Cortex February 2008;18:344-363
doi:10.1093/cercor/bhm059
Advance Access publication May 20, 2007

# Embryonic and Postnatal Development of the Layer I–Directed ("Matrix") Thalamocortical System in the Rat

Maria J. Galazo, Verónica Martinez-Cerdeño, César Porrero and Francisco Clascá

Department of Anatomy & Neuroscience, School of Medicine, Autónoma University, E-28871 Madrid, Spain

**Inputs to the layer I apical dendritic tufts of pyramidal cells are crucial in "top-down" interactions in the cerebral cortex. A large population of thalamocortical cells, the "matrix" (M-type) cells, provides a direct robust input to layer I that is anatomically and functionally different from the thalamocortical input to layer VI. The developmental timecourse of M-type axons is examined here in rats aged E (embryonic day) 16 to P (postnatal day) 30. Anterograde techniques were used to label axons arising from 2 thalamic nuclei mainly made up of M-type cells, the Posterior and the Ventromedial. The primary growth cones of M-type axons rapidly reached the subplate of dorsally situated cortical areas. After this, interstitial branches would sprout from these axons under more lateral cortical regions to invade the overlying cortical plate forming secondary arbors. Moreover, retrograde labeling of M-type cell somata in the thalamus after tracer deposits confined to layer I revealed that large numbers of axons from multiple thalamic nuclei had already converged in a given spot of layer I by P3. Because of early ingrowth in such large numbers, interactions of M-type axons may significantly influence the early development of cortical circuits.**

**Keywords:** axon branching, motor cortex, somatosensory cortex, thalamostriatal, VGluT2

## Introduction

The pyramidal neurons apical dendritic tufts in cortical layer I are now recognized as the key synaptic site for top-down interactions in cortical networks (Cauller 1995; Ichinohe and Rockland 2004; Larkum et al. 2004; Shlosberg et al. 2006). A distinct population of thalamocortical relay cells, the "matrix" cells (M-type cells, Jones 2001), selectively targets the apical dendritic tufts in layer I (Herkenham 1986; Arbuthnott et al. 1990; Lu and Lin 1993; Castro-Alamancos and Connors 1997; Jones 2001; Thomson and Bannister 2003), and may thus mediate top-down interactions via the thalamus (Deschênes et al. 1998). Besides, the observation that M-type cells are widely distributed in the thalamus and often innervate the cortex in a highly convergent/divergent manner (Avendaño et al. 1985, 1990; Herkenham 1986; Rieck and Carey 1985; Jones 2001) led to the proposal that they might be a substrate for the synchronization of widely distributed neuronal ensembles. Such synchronization is believed to underlie cognitive events (Jones 2001; Llinás et al. 2002).

The M-type relay cells and their axons are anatomically and functionally different from the well-known "Core" relay neurons (C-type, Jones 2001) that innervate cortical layer IV. M-type cells do not arborize in layer IV and C-type cells do not arborize in layer I. Additionally, M-type cell axons may also arborize in layer Va, which is not targeted by C-type axons (Herkenham 1986; Deschênes et al. 1998). M-type axons frequently innervate wide tangential domains of the cortex, often including multiple cortical areas (Lorente de No 1938; Ferster and LeVay 1978; Macchi et al. 1996; Deschênes et al. 1998; Monconduit and Villanueva 2005), whereas most C-type axons arborize topographically within single areas, usually in very localized domains (Jones 1985; Bernardo and Woolsey 1987; Jensen and Killackey 1987; Sur et al. 1987; Garraghty and Sur 1990; Rausell et al. 1998). In some nuclei, M-type and C-type cells have been shown to differ in mean soma size (Carey et al. 1979; Penny et al. 1982; Rausell and Avendaño 1985; Avendaño et al. 1985, 1990) or in their expression of calcium-binding proteins (Jones and Hendry 1989; Cruikshank et al. 1991; Hashikawa et al. 1991; Rausell and Jones 1991; Lin et al. 1996).

M-type neurons predominate in extra-lemniscal sensory, motor, association, and limbic nuclei, whereas C-type neurons prevail in the "lemniscal" sensory nuclei of the thalamus (Herkenham 1986; Rieck and Carey 1986; Jones 2001; Rubio-Garrido et al. 2004). In the nuclei in which they coexist, C-type and M-type cells are segregated into different cell clusters or layers that receive different inputs (Jones and Hendry 1989; Rausell and Jones 1991; Boyd and Matsubara 1996; Jones 2001).

In development, interactions between ingrowing thalamocortical axons and cortical neurons are central for the specification and fine-tuning of cortical circuits (reviewed in Sur and Rubenstein 2005). Because of their abundance and specific laminar targeting, M-type axon interactions with developing cortex might well be significant, and probably unique. However, despite the wealth of studies that have examined thalamocortical development, virtually nothing is known about the development of these M-type axons. This void is partly because previous studies focused mainly on nuclei such as the ventroposterior (Wise and Jones 1977; Erzurumlu and Jhaveri 1990, 1992; Senft and Woolsey 1991; Agmon et al. 1993, 1995; Catalano et al. 1996; Marotte et al. 1997; Auladell et al. 2000) or the dorsal lateral geniculate (Lund and Mustari 1977; Sheng et al. 1991; Ghosh and Shatz 1992; Kageyama and Robertson 1993; Miller et al. 1993; Molnár et al. 1998), which happen to contain few or no M-type cells. As a result, the topographically layer IV–directed C-type axons are today the only paradigm for molecular and genetic studies of thalamocortical development (recent reviews in López-Bendito and Molnár 2003; Garel and Rubenstein 2004; Price et al. 2006).

Precise temporal and spatial data on the developmental steps of thalamocortical axon growth are necessary to understand the actual "in vivo" effect of candidate regulatory mechanisms (Skaliora et al. 2000; Dufour et al. 2003; Lopez-Bendito et al. 2006). However, the time course of M-type thalamocortical axon development is unknown. For example, it is unclear how and when a single axon grows and begins to selectively target

multiple separate areas. Likewise, the timing of M-type axon arborization into layer I remains uncertain. Fragmentary observations in primates (Rakic 1977), carnivores (Kato et al. 1983, 1986; Kawaguchi et al. 1983; Shatz and Luskin 1986; Noctor et al. 2001), and marsupials (Sheng et al. 1991; Marotte et al. 1996) indicated that at least some thalamic axons arborized in layer I days before thalamic axon arbors begin to develop in the middle cortical layers. Tracer studies in rodents have not yielded comparable observations (Kageyama and Robertson 1993; Miller et al. 1993; Catalano et al. 1996). In the adult, M-type axons arising in multiple thalamic nuclei are known to converge in layer I of a given cortical site (Parnavelas et al. 1981; Rieck and Carey 1985; Herkenham 1986; Clancy and Cauller 1999); however, it is still not known how and when convergence occurs during development.

We set out to examine the timing of M-type axon extension, branching, and lamina-specific arborization in embryonic and postnatal rats. We focused on the axons arising from 2 thalamic nuclei, the Posterior (Po) and the Ventromedial (VM), which are predominantly composed of M-type neurons in rats (Herkenham 1986; Lin et al. 1996; Deschênes et al. 1998; Rubio-Garrido et al. 2004), and which innervate multiple areas over extensive swaths of the cerebral hemisphere (Herkenham 1979, 1986; Deacon et al. 1983; Condè et al. 1990; Wang and Kurata 1998; Linke 1999; Desbois and Villanueva 2001). Results reveal the timing and developmental steps followed by M-type axons to target, innervate, and arborize within multiple areas in layer I.

## Materials and Methods

### *Surgical and Anesthetic Procedures*

A total of 189 fetal (E16–E22) or postnatal (P0–P30) albino Wistar rats were examined in this study. For some techniques, brains were midsagittally split and each hemibrain then used in independent experiments. The total numbers of valid experimental cases at each age, on which the following account is based, are listed in Table 1.

All procedures involving animals were carried out in accordance with European Community Council Directive 86/609/EEC guidelines and were approved by the University's Bioethics Committee. Fetal animals were obtained from time-mated (12-h mating period) dams. The time of mating was considered the first embryonic day (E0). With this designation for embryonic days, gestation lasted 22 days, and the day of birth, "E23," was designated as P0.

**Table 1**
Valid cases studied with each axonal tracing technique

| | DiI (fixed tissue) | Biocytin (ex vivo) | BDA (in vivo) | FB (in vivo) |
|---|---|---|---|---|
| E16 | 6 | 2 | | |
| E17 | 6 | 5 | | |
| E18 | 9 | 5 | | |
| E19 | 7 | 5 | | |
| E20 | 6 | 2 | | |
| E21 | 7 | 8 | | |
| E22 | 6 | 2 | | |
| P0 | 5 | 10 | | 3 |
| P1 | 8 | 4 | 6 | 8 |
| P2 | 4 | 1 | 5 | 8 |
| P3 | 8 | | 7 | 6 |
| P4 | 3 | | 6 | 8 |
| P5 | | | 5 | 8 |
| P6 | 7 | | 8 | |
| P7 | | | 2 | |
| P9 | | | 5 | |
| P12 | | | 4 | |
| P15 | | | 2 | |
| P30 | | | 2 | |

Note: Developmental ages indicate the day of brain fixation.

Early postnatal animals (P0–P5) were anesthetized with deep hypothermia by placing them in ice-cold saline. Older postnatal animals were anesthetized with a ketamine (Ketolar®, Parke-Davis, Madrid, Spain 0.375 mg/10 g, s.c.)–xylacine (Rompun 0.1 mg/10 g, s.c.) combination, or with isofluorane 1–2% in oxygen. Prenatal animals were obtained from pregnant dams deeply anesthetized with a combination of ketamine (66 mg/kg, i.p.) and xylacine (8 mg/kg, i.p.), fetuses were extracted by cesarean section and immediately immersed in ice-cold saline, before processing for "ex vivo" microinjection or DiI labeling (see below).

### *DiI Tracing in Fixed Brains*

Fetal brains used for tracing studies with DiI (1,1′-dioctydecyl-3,3,3′,3′-detramethyl-indocarbocyanine) were fixed by immersion in 4% paraformaldehyde in phosphate buffer (PB) pH 7.4 for 48 h. Postnatal animals were fixed by perfusion with a mixture of 4% paraformaldehyde in 0.1 M PB for 5 min through a 26-gauge hypodermic needle inserted into the left ventricle. After dissection and removal from the skull, the brains were postfixed for 24 h in the same fixative, and subsequently transferred to 0.1 M PB with 0.1% sodium azide. Under a dissecting microscope, small (25–50 μm diameter) crystals of DiI were inserted in the brains using needle tweezers or insect pins. On midsagittally split brains, crystals were inserted under direct visual guidance in VM. Similarly, after coronally sectioning the diencephalon at the level of the habenula, crystals were implanted in Po. The exact implant sites were verified at the end of the experiment from the serial brain sections (Fig. 1*A*,*B*).

Implanted brains were stored at 27 °C in the dark for 3 weeks to 3 months, depending on age, in 0.1% sodium azide in 0.1 M PB. Subsequently, brains were embedded in 2% agarose (Type 1A, Sigma-Aldrich, Madrid, Spain), and serially sectioned in the coronal plane on a Vibratome into 100-μm-thick sections. Sections were stored, free-floating, in PB at 4 °C. For microscope examination, the sections were temporarily wet-mounted on glass slides. Sections were bisbenzimide-counterstained for cytoarchitectonic reference.

### *Biocytin Microinjections in Whole Brains Maintained Ex Vivo*

Biocytin was used to anterogradely label small groups of M-type axons. We modified a protocol for biocytin microinjections in whole brain hemispheres maintained "ex vivo" (Chang et al. 2000). Embryonic (E16–E22) or postnatal (P0–P3) brains were dissected out from the skull in oxygenated artificial cerebrospinal fluid (ACSF: NaCl 137 mM; KCl 5 mM; $CaCl_2$ 2 mM; $MgCl_2$ 1 mM; $NaH_2PO_4$ 2 mM; D-glucose 10 mM; pyruvic acid 10 mM; 4-(2-hydroxyethyl)-1-piperazineethanesulfonic acid 5 mM) pH 7.35 at 4 °C. Brains were then split in the midsagittal plane. Each hemisphere was transferred to a slice-recording chamber with a constant flow of oxygenated ACSF at 22 °C. Under a dissecting microscope and cold-light illumination, the intended area of injection was identified using tissue landmarks. A glass micropipette (3–15 μm external tip diameter) containing a solution of 2% biocytin (Sigma, St Louis, MO) in 0.5 M potassium acetate was lowered into the thalamus through the midsagittal surface of the split brain under visual guidance. The tracer was iontophoresized by passing a positive current of 600 nA–1 μA at a frequency of 1 Hz for 10–15 min, and the pipette was then removed. To allow for axonal transport, the brain hemispheres were placed into a container with ACSF at 22 °C where a mixture of 5% $CO_2$ and 95% oxygen was continuously bubbled for 4–8 h. Subsequently, the hemispheres were fixed by immersion in 4% paraformaldehyde in phosphate-buffered saline 0.1 M for 48 h. Hemispheres were then embedded in 2% agar (type VII, Sigma) in saline, and vibratome-sectioned in the coronal plane at 100 μm. All the serial sections were mounted in the order of cutting on gelatin-coated slides, and air-dried.

A standard streptavidin–peroxidase protocol with ammonium nickel sulfate enhancing was used to reveal biocytin. Sections were lightly counterstained with thionin for cytoarchitectonic reference, briefly dehydrated in graded alcohols, cleared in xylene, and coverslipped with DePeX.

### *"In Vivo" Microinjections of Biotinylated Dextrans in the Thalamus*

In vivo microinjections of lysine-fixable 10 000 MW biotinylated dextran amine (BDA) were used to label M-type axons in postnatal animals. Animals were anesthetized as described above, and then placed in a stereotaxic apparatus adapted for neonatal rodents (David Kopf

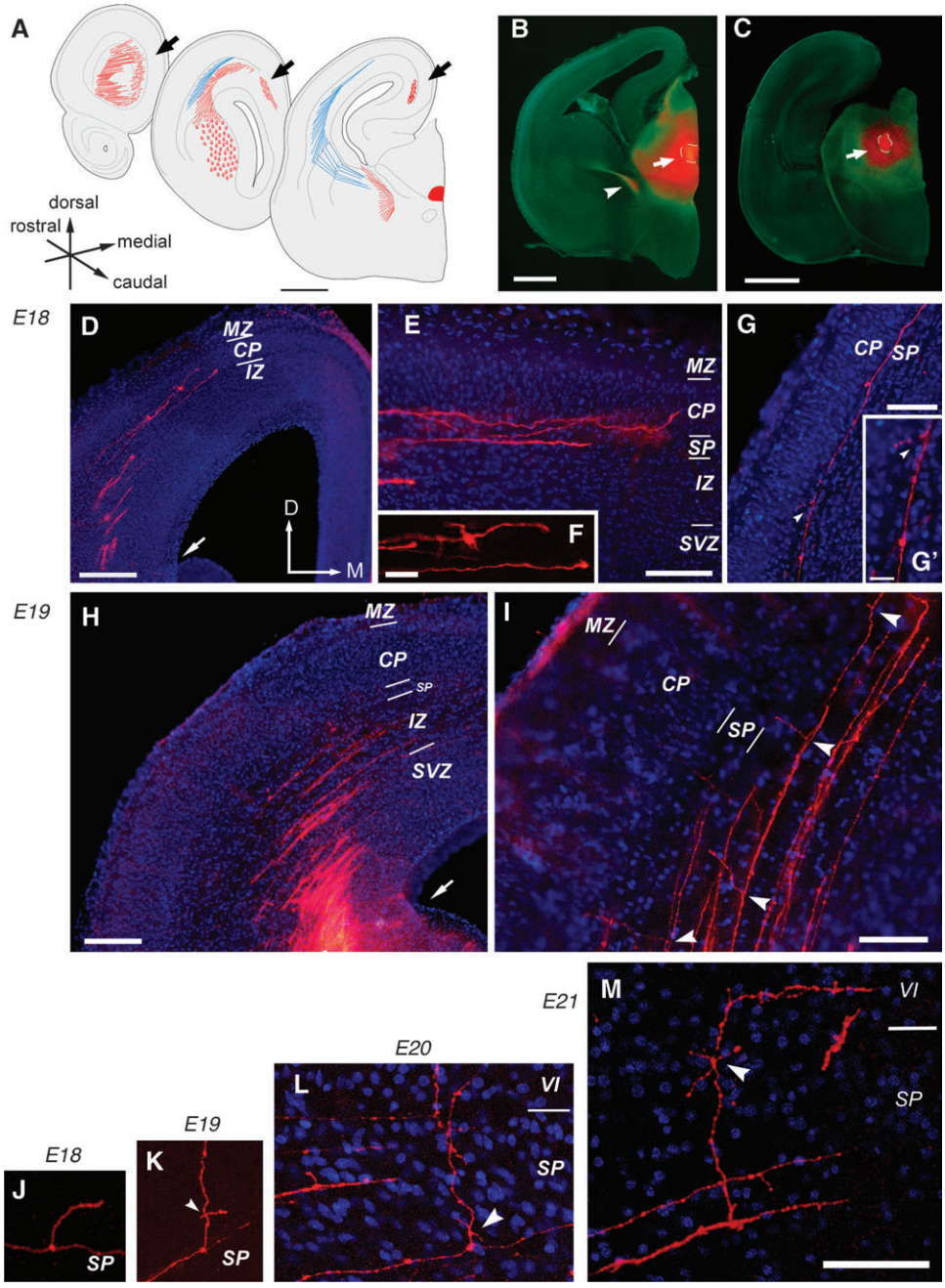


**Figure 1.** Labeling of developing M-type axons with DiI tracers in embryonic rats. (*A*) Schematic representation of the trajectory and general distribution of labeled axon tracts after DiI deposits in the VM (in red) or in the Po (in blue) thalamic nuclei. On the left, the trajectories of these 2 bundles of labeled fibers are schematically represented on 3 sections of an E21 cerebral hemisphere. Note the labeled fibers turning around the rostral pole of the cerebral ventricle and running caudally in the cingulum bundle (arrow). (*B*, *C*) Examples of injection sites in VM at E18 (panel "*B*") or Po at E21 (panel "*C*"). Images were acquired under epifluorescence illumination through a filter set that allows visualization of the crystal implants (arrowheads), while dampening the intense labeling of surrounding thalamic tissue. Note in "*B*" the tight bundle of labeled fibers traversing the MGE (arrow). (*D*) Labeled axons growing into the presumptive frontoparietal cortex after a VM deposit at E18. Note the dispersion of these axons in the radial (deep-to-superficial) dimension of the pallium. Note the large primary growth cones at the distal end of the axons. (*E*) Primary growth cones of thalamocortical axons growing tangentially in the SP and IZ of the dorsal pallium after a deposit in Po at E18. Although most cones are oriented tangentially to the pallial layers, a cone in SP is turned toward the overlying CP. (*F*) High-magnification detail of some highly complex, often ramified, growth cones observed on axons extending tangentially in SP at E18. Because shape and size of growth cones is known to change as they cross different cellular and extracellular substrates (Halloran and Kalil 1994; Catalano et al. 1996), it is to be kept in mind that the morphology observed in these particular cones represents just a snapshot of structures that are highly dynamic. (*G*, *G'*) A short interstitial branch can be seen sprouting from a labeled axon running under the lateral parietal CP. Note that the sprouting is located hundreds of microns from the primary growth cone of the axon. (*H*) Labeled axons in the dorsolateral frontoparietal cortex after a VM deposit in an E19 brain hemisphere. Note that axons can be seen navigating the SP, IZ, and SVZ. (*I*) In the same experiment as panel "*H*," most axons tangentially navigating the SP and superficial IZ of the lateral zone of the pallium have grown short branches directed toward the CP. (*J*–*L*) Growth of interstitial axon branches labeled in the dorsolateral cortex after VM deposits at E18 ("*J*"), E19 ("*K*"), and E21 ("*L*"). In panels "*K*" and "*L*," note the presence of small secondary sproutings on the branches. Bars *A* = 1 mm; *B*, *C* = 500 μm; *D*, *H* = 250 μm; *E*, *G*, *J* = 100 μm; *F* = 50 μm; *G'* = 25 μm; *J*–*M* = 75 μm.

Instruments, Tujunga, CA). The pup's head was gently stabilized in position with special pup earbars and plasticine. Under a surgical microscope, a midsagittal incision was made in the scalp, and a small piece of the parietal bone was cut and removed with a scalpel. The dura mater was punctured, and a micropipette containing BDA 10 000 MW Molecular Probes 1% in 0.5 M potassium acetate pH 7.4 was vertically lowered into the thalamus with the stereotaxic holder. For each age, the "stereotaxic" injection coordinates were derived from in-house atlases elaborated from series of fresh, coronally sectioned brains of the same age. Square pulses of 1–2 μA, 7 s on/off, were applied using a Midgard current source (Stoelting, Wood Dale, IL) for 10 min. The micropipette was removed, the bone piece was repositioned and fixed with cyanoacrylate glue, and the skin sutured. After recovering from anesthesia, the pups were returned to their mothers and allowed to survive for 1–2 days. The pups were then sacrificed and perfused as described for the DiI experiments. After removal from the skull, brains were soaked for 48 h in 30% sucrose in PB, and embedded in a 2% agar block made with the same sucrose solution. The block was coronally sectioned on a freezing microtome at 50 μm. Sections were then processed to reveal BDA with a standard avidin–biotin–peroxidase method, mounted on gelatin-coated glass slides, air-dried, counterstained, and finally dehydrated and coverslipped as described.

### *Epidural Applications of Fast Blue*

The location in the thalamus neurons innervating layer I was determined by applying the retrograde tracer Fast Blue (FB, diamidino compound 253/50, Dr Illing GmbH & Co. KG, Groß-Umstadt, Germany) on the cortical surface. Postnatal (P0–P5) and E22 pups delivered by cesarean section on the last day of gestation were used for these experiments (Table 1). Under hypothermic anesthesia, the skull was opened as described above. A minute piece (<0.5 × 0.5 mm) of Whatman filter paper dried after soaking in 0.2% FB in distilled water was gently placed over the dura mater overlying the dorsal frontoparietal cortex. The paper was left in place, and the bone was closed with the same bone fragment that had been previously removed. The animals were reheated, and returned to the dam, except in the case of the E22 animals, which were kept in a high-humidity chamber at 37 °C and given periodic glucose/saline saline subcutaneous injections until sacrifice 24 h after delivery. Animals were sacrificed after 24–48 h of survival, and perfused as described for the DiI experiments. The brains were included in 2% agar in PB + 30% sucrose, coronally sectioned in a freezing microtome, and immediately mounted onto gelatin-covered glass slides. Finally, the tissue sections were dehydrated and coverslipped with DePeX.

### *Immunobistochemistry*

Paraformaldehyde-fixed serial coronal 50-μm-thick sections from fetal and postnatal animals were assayed with an antibody against the type 2 vesicular glutamate transporter (VGluT2; 1:2500, Chemicon, Temecula, CA), as a selective marker of presynaptic thalamocortical specializations. Immunolabeling was revealed on free-floating sections following standard protocols using ABC kits (Vectastain, Vector Laboratories, Burlingame, CA). Sections were then dehydrated and coverslipped.

### *Microscope Analysis and Imaging*

Sections were examined and imaged using a Nikon Eclipse 600 microscope with a Prior Proscan (Prior Scientific Instruments, Cambridge, UK) motorized stage, a DMX1200 digital camera, and a computerized imaging system (AnalySIS® 3.1, Soft Imaging System GMBH, Munster, Germany) able to control both image acquisition and stage motion. Sections labeled with DiI or FB were examined at 40–400× under a 100-W Hg light source with wide diameter Nikon objectives. In FB experiments, we routinely acquired the images of 10–20 adjacent fields of the thalamus or cortex at 100–200×, and fused them in a single panoramic high-resolution mosaic image file with the Multiple Image Alignment module of the AnalySIS® software (Supplementary Fig. SM3). Examination and plotting of FB-labeled cells was carried out on these mosaic image files with Canvas X software (ACD Systems, Saanichton, BC, Canada) on Apple G4 computers. This digital procedure allowed a thorough examination and precise recording of each labeled neuron without photobleaching.

Selected axons were reconstructed in serial sections with a camera lucida and a neurolucida system (MicroBrightField, Magdeburg, Germany) mounted on a Nikon microscope. In addition, we often acquired several images of the same field at different depths in the *z*-axis and then fused them in a single image of the labeled axons applying the Extended Focal Imaging module of the AnalySIS® software. On the reconstructed axons, the mean number of branching points in the subcortical white matter, mean total axon length per intracortical arbor, and leading growth-cone progression into the developing cortical plate (CP) were calculated for the various ages in a total of 51 axons (minimum 5 axons per age).

DiI or bisbenzimide fluorescence images were serially acquired though different filter sets and digitally overlaid on a single image. We also examined selected sections with a Leica TCS SPII spectral confocal microscope using an Ar/He/Ne (543 nm) laser line. Stacks of serial 1-μm-thick optical slices on the *z*-axis were averaged in a single "flat" image applying the Kalman filter of the Leica software.

The DAB-labeled sections were examined and imaged at 40–1000× using high aperture plan-apochromatic Nikon objectives. Image processing consisted only of adjustments in tone scale and gamma as needed to obtain optimal images. Canvas software was employed for final figure composition. For delineation of brain structures and nomenclature, we used embryonic rat (Foster 1998) and adult rat (Paxinos and Watson 1998) brain atlases. In describing the cellular layers in the developing rat cortex we employed the nomenclature detailed by Kageyama and Robertson (1993) in their studies of the visual cortex.

### *Overview*

We examined the developmental time course of axons arising from Po or VM thalamic nuclei, which consist mainly of M-type neurons (Herkenham 1986), in rats aged E16–P30.

Anterograde labeling after thalamic deposits of DiI, Biocytin, or BDA revealed that the primary growth cones of M-type axons first reach the subplate (SP) of dorsally situated target areas before sprouting interstitial branches under more lateral cortical regions; these branches then invade the overlying CP and become secondary arbors. Advancing of M-type growth cones slows twice before extending tangentially under the pia. The first delay occurs in the infragranular layers and last about 4 days and the second occurs in the lower part of layer I for about 2 days. Subpial extension and branching of M-type axons is largely restricted to the outer part of layer I (sublayer Ia) from the start.

In addition, deposits of FB in layer I of the dorsal sensorimotor cortex were used to retrogradely label the whole population of thalamocortical cells whose axons had already reached layer I by a given postnatal age. These experiments revealed that, as early as P3, the axons of a great many M-type neurons located in multiple thalamic converge into a relatively small single spot of the dorsal sensorimotor layer I.

### *DiI Labeling of Axons after Crystal Implants in the Thalamus*

In embryonic brains, DiI fluorescence after crystal implants in VM or Po nuclei revealed thalamocortical axons up to their terminal growth cones with Golgi-like detail (Figs 1 and 2). These experiments showed the overall topography of the thalamocortical pathways originating in each nucleus. Moreover, in peripheral parts of the bundle, the morphology of individual axons could be observed within single sections. After deposits in Po or in VM, the labeled axon bundles occupied different positions in the corona radiata. Labeled Po axons extended along the central part of the internal capsule and then arched under the lateral cortex en route to a dorsal zone of the hemisphere (Fig. 1*A*). In contrast, labeled VM axons first extended toward the frontal pole in the anteroventral part of the internal capsule and then around the rostral end of the

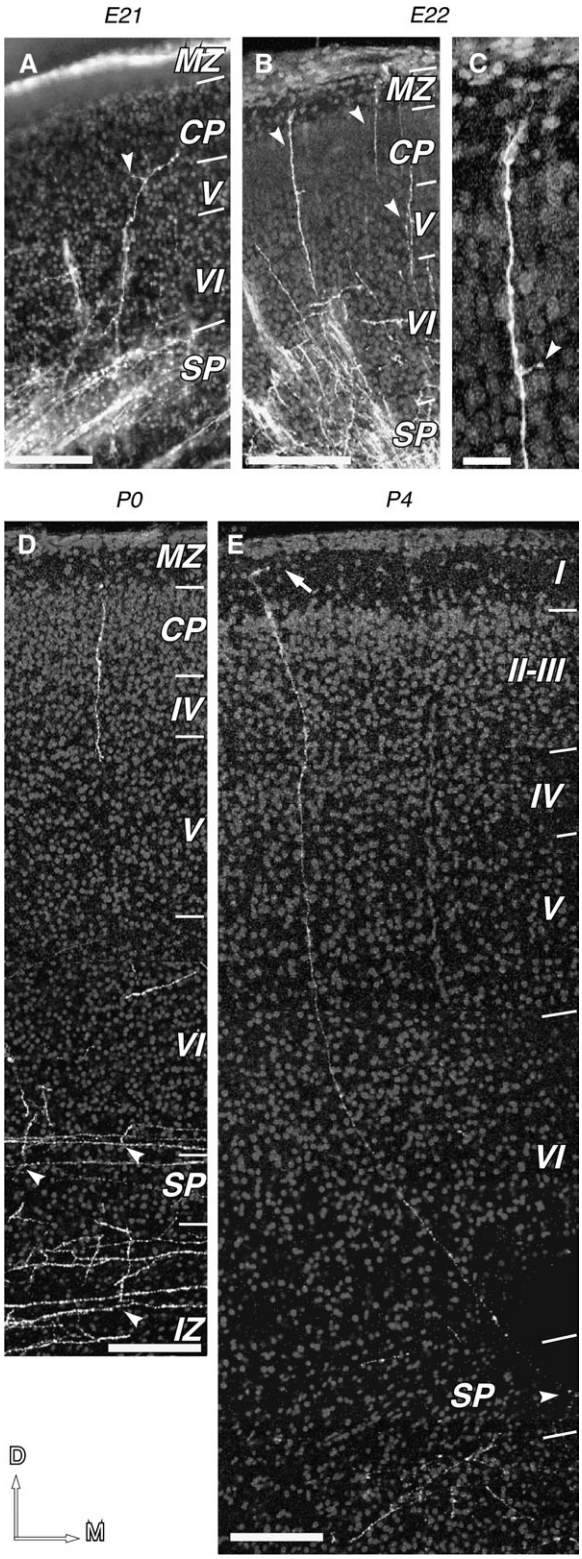


**Figure 2.** DiI-labeled thalamic matrix axons growing toward the marginal zone (MZ)/layer I (I, top) in the parieto-frontal cortex of E21–P2 brains after implants in the Po nucleus. (*A*) E21. An obliquely growing axon has reached the inner border of the dense CP. A small secondary branch emerges from it (arrowhead). (*B*, *C*) E22. Following mainly radial trajectories, a few growth-cone tipped axons reach the inner part of the marginal zone/layer I at this early age. Note that they are mostly simple and radially oriented, but occasionally show small branchlets in deeper layers (indicated with and arrowhead in the higher magnification detail in panel "*C*"). (*D*) P0. At this age, axons reaching layer I do not branch or extend tangentially within this layer. In SP and IZ, a number of axons with collateral branching points (arrowheads) can be seen. (*E*) P4. An axon extending from a branching point in SP (arrowhead) to layer I can be followed in a single 100-μm-thick section. After a 90° turn several microns under the pial surface the branch continues tangentially out of this coronal section (arrow). Most Po axons have already sprouted branches in layer V at this age, but this particular one had not. Bars $A = 100$ μm; $B$, $D$, $E = 150$ μm; $C = 25$ μm. *A* is a standard epifluorescence image, *B*–*E* are confocal microscope images. Abbreviations as in Figure 1.

lateral ventricle. Some VM axons continued caudally under the dorsomedial cortex in the nascent cingulum bundle. Despite these general topographic differences, the Po and VM labeled axons developed at similar paces; for brevity the DiI labeling-observations of axons from the 2 nuclei are described together below.

By E17, a compact bundle of axons had extended rostrolaterally across the developing reticular thalamic nucleus and then turned laterally to traverse the medial ganglionic eminence (MGE, future globus pallidus) through a narrow corridor. Further along, the axon bundle had dispersed into numerous small bouquets of a few axons in the mantle layer of the lateral ganglionic eminence (LGE, future striatum) and crossed the pallio-subpallial boundary (López-Bendito and Molnár 2003) into the pallium. In the deep pallial layers, axons were seen navigating parallel trajectories, but widely dispersed in the radial dimension: some navigated along the upper intermediate zone (IZ) and SP, whereas others extended either in the IZ or through the subventricular zone (SVZ). The most advanced primary growth cones of these axons were found in the IZ of the lateral part of the dorsal pallium (not illustrated). Note that, although labeled axons at this age did not show branches, we refer to their leading growth cones as "primary" (Szebenyi et al. 2001), to distinguish them from the cones that appear in the higher-order branches that sprout at later ages (see below).

By E18, some primary cones of labeled Po axons were already present in the dorsomedial zone of the hemisphere. Similarly, VM primary growth cones had reached the frontal pole, but none were yet seen in the cingulum bundle. In both cases, the growth cones were large (50–150 μm) and highly complex (Fig. 1*D*,*E*). In the deep pallial layers, the tangential trajectory was slightly tilted toward the surface, so that the primary growth cones eventually emerged into the SP. At the point where the SP was reached, most primary growth cones turned abruptly toward the overlying cell-dense CP, but some continued for few hundred microns along the SP before finally entering the CP. Labeled axon trunks were still essentially unbranched at E18; although there were a few very short (<50 μm long) processes directed toward the CP from some of the trunks (Fig. 1*F*). These branchlets were observed in axon zones situated under the lateral part of the dorsal pallium, many hundreds of microns away from the primary cone.

In E19 brains, Po axon growth cones remained in the dorsomedial frontoparietal cortex. Meanwhile, some labeled primary cones from VM axons had extended back around the frontal pole of the lateral ventricle, and were navigating in the cingulum bundle. Axons from Po and VM exhibited relatively short (<200 μm) branches that sprouted at the level of the SP and upper IZ. All of these branches were directed to the CP and had reached the deep cell rows of the CP (Fig. 1*K*) which will become layer VI (Bayer and Altman 1991).

Over the following 5 days (E21–P2), the length of branches in the DiI-labeled axons increased steadily. These branches began

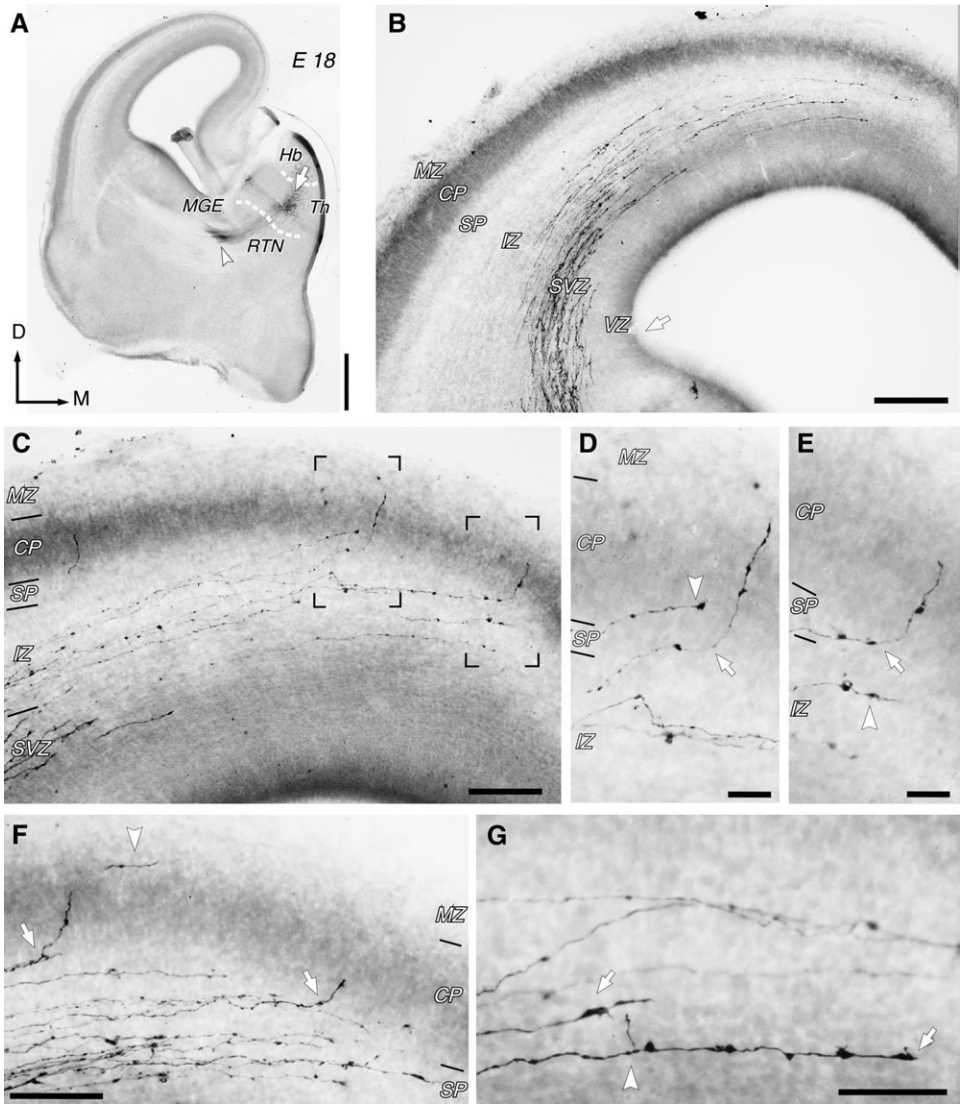


**Figure 3.** Labeling of developing thalamic matrix axons after a biocytin iontophoretic microinjection in an E18 hemibrain + 5 h "ex vivo." (*A*) Thionin-counterstained coronal section through the center of the injection site. The small injection site (arrow) is situated in the prospective VM/ventrolateral nuclei region. Note also a bundle of thalamic radial glia labeled from the injection site. In this section, the bundle of labeled thalamocortical axons (arrowhead) can be seen turning laterally into the Medial ganglionic eminence (MGE). (*B*) Labeled axons extend tangentially along the deep pallial layers. Notice that despite originating in a small thalamic domain, these axons are widely dispersed in the radial dimension of the pallium. (*C*) A more rostral section from the same case. Observe that, as in panel "*B*," the deepest axons, which are directed toward dorsomedial pallial zones, extend in the SVZ zone in the lateral part of the pallium. (*D*, *E*) High-magnification detail of the insets in panel "*C*." In each panel, a primary growth cone that has reached the SP has turned toward the pial surface (arrows). In contrast (panel "*D*"), another growth-cone tipped axon (arrowhead) follows a tangential trajectory in the deep cellular tiers of CP. (*F*) Dorsal convexity of the frontal pallium in the same experiment. Note the large primary growth cones of the axons. Arrow indicate 2 axons that have turned toward the CP. The one on the left, has even entered and extended a growth cone into the marginal zone. Note that the CP is still thin here. (*G*) High-magnification view of the large, complex primary growth cones (arrows) of M-type axons navigating tangentially in the IZ. An occasional branch (arrowhead) can be seen sprouting perpendicularly from an axon in the upper IZ, not far from its primary growth cone. Bars: $A = 500$; $B = 250$ μm; $C$, $F = 200$ μm; $D$, $E = 25$ μm; $G = 50$ μm. Abbreviations: RTN, reticularis thalami nucleus; Th, dorsal thalamus; Hb, habenula. Other abbreviations as in Figure 1.

showing some second or even third order divisions, which arose mainly in SP and the deepest parts of CP (Fig. 1*J*,*M*), but, overall, they remained relatively simple. Branches were tipped by relatively small (<25 μm) growth cones and had radial or oblique trajectories. Together, these branches formed a very loose and irregular "wavefront" of labeled cell processes. Comparison of the axons labeled at different ages suggests that these branches progressed rather slowly toward the cortical surface (Fig. 2*A*). From P0 onwards, isolated axon branches were first seen extending all the way up to layer I (Fig. 2*B*,*C*). These branches were often undivided as they traversed the CP, and many of them had no branches in deeper layers, either (Fig. 2*E*). Most of the branches reaching layer I were radially oriented, although some had oblique trajectories. In P1–P2 animals, branches reaching layer I were more numerous but, remarkably, the growth cones at the tip of all the branches remained radially or obliquely oriented, and at some distance under the pia (Fig. 2*B*,*C*). In P3–P6 animals, most of the growth cones labeled in layer I had taken an abrupt turn, and extended tangentially for some distance under the piamater (Fig. 2*E*).

In addition to branches extending up to the pial surface, axons labeled between E21–P3 showed other branches that did not extend beyond layers V and VI.

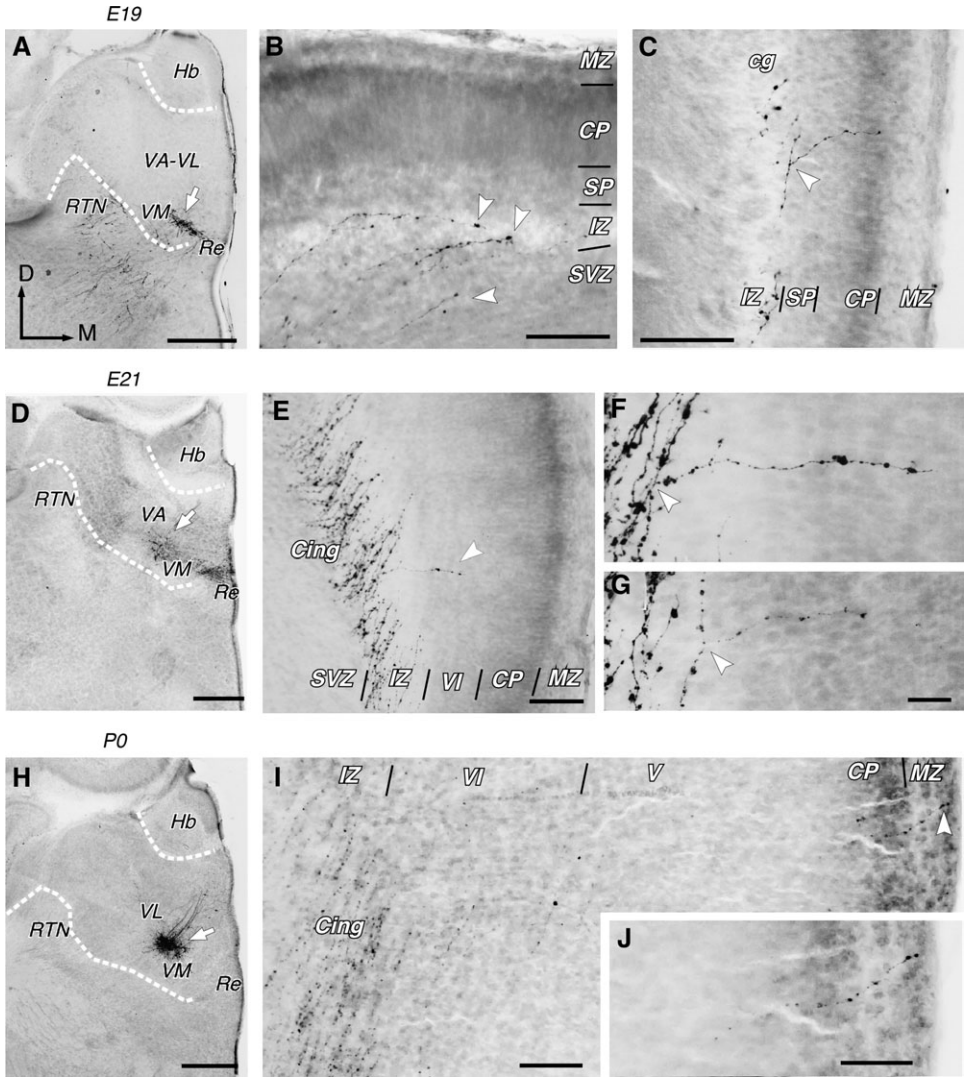


**Figure 4.** Thalamocortical axons labeled after biocytin microinjections in the VM nucleus of E19–P0 hemibrains "ex vivo." Panels *A*, *D*, and *H* illustrate coronal sections taken at the core of the injection sites (arrows) corresponding, respectively, to E19, E21, or P0 hemibrains. Thionin counterstain. (*A–C*) Labeling in an E19 + 6 h "ex vivo" hemibrain. In panel "*B*," axons are shown as they run in the IZ and SVZ of the dorsal frontal cortex. Their large primary growth cones are indicated with arrowheads. Panel "*C*" shows axons running tangentially in the SP of the cingulate cortex (prospective cingulum bundle). In panels *C*, *E–G*, and *I*, *J*, the direction of axons labeled in the cingulum is almost perpendicular to the coronal plane. Nevertheless, sizable axonal segments can be visualized because these coronal sections were relatively thick (100 μm). In panel "*C*" an interstitial branch from an axon trunk can be seen extending radially into the CP. (*D–G*) E21 hemibrain + 6.5 h "ex vivo." Numerous axons can be seen running in the cingulum (Cing). One of them gives a branch (arrowhead) that radially invades cortical layer VI. A detail of this branch is shown in panel "*F*," and a similar branch is shown in "*G*." Note that the growth cones of some of these branches have passed the inner border of CP. The beadlike appearance of the labeled axons was common in the experiments conducted with "ex vivo" perinatal hemibrains; it may have resulted from the prolonged survival of the tissue under hypoxic conditions. (*H–J*) P0 + 6 h "ex vivo" hemibrain. Axons labeled in the cingulum and a radial branch whose growth cone has reached the MZ. The branching point was in a nearby section (not shown). A higher magnification detail of the growth cone (arrowhead in "*I*") is seen in panel "*J*." Bars: *A*, *D*, *H* = 1 mm; *B*, *C*, *E*, *I* = 100 μm; *F*, *G* = 25 μm; *J* = 50 μm. Abbreviations: Hb, habenula; Re, reuniens nucleus; RTN, reticular thalamic nucleus; VA, ventral anterior nucleus; VL, ventrolateral nucleus. Other abbreviations as in Figure 1.

The ability of DiI to label axons in layer I decreased rapidly after P3–P4, even with longer incubation times (up to 3 months at 27 °C). Labeling of intracortical axon branches became fainter and progressively more diffuse, rendering the technique unreliable in older animals.

### *''Ex Vivo'' Iontophoretic Biocytin Microinjections in Whole Brain Hemispheres*

To confirm the observations based on the passive diffusion of DiI as well as to allow the selective labeling of small of groups of M-type axons along their entire trajectory from thalamus to cortex, we applied biocytin iontophoretic microinjections in whole brain hemispheres cultured "ex vivo." These experiments produced injection sites of 100–200 μm in diameter, consisting of just a few dozens of labeled somata, which we interpret as the somata that originated the labeled axons. A small bundle of diencephalic radial glia cells was usually labeled as well (Fig. 3*A*). Developing thalamocortical axons were continuously stained from the injection site in the thalamus to their growth cones.

Biocytin injections in Po or VM at E16 and E17 labeled a small bundle of axons that extended in the deep pallial layers following parallel but mostly independent trajectories. By E18, the most advanced primary growth cones had reached the

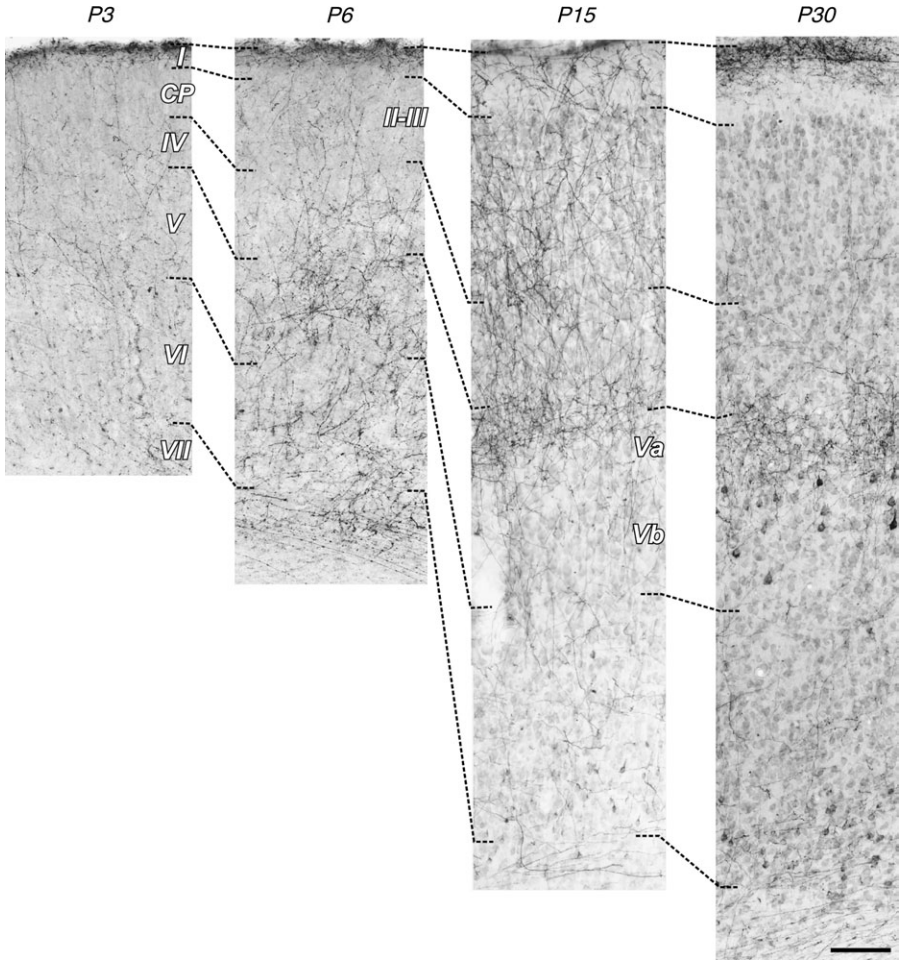


**Figure 5.** Postnatal (P3–P30) development of axons from the Po nucleus in the somatosensory cortex. Columnar samples of SI sections extending from the pial surface (top) to the white matter. Axon arbors labeled after stereotaxic iontophoretic BDA deposits in the thalamus can be seen against a light thionin counterstain. Note that cortical layers differentiate and expand considerably over this period. Observe that, with age, the labeled thalamic arbors progressively accumulate in sublayers Ia and Va. The injection sites in these experiments are shown in Supplementary Material Figure SM2. Although all injections were located in the medial portion of Po, they involved slightly different coronal levels; thus, it cannot be ruled out that, in addition to the actual developmental changes, the different levels of the injection sites within Po may have contributed subtle differences in these axonal arbor patterns. Bar = 100 μm.

dorsalmost part of the cerebral vesicle (Fig. 3*B*). Axon trajectories in IZ and SVZ bent toward the pallial surface that eventually led them into the SP. Because of the small number of labeled axons, it was readily evident that the points at which these distal tips reached the SP were roughly correlated with their superficial-to-deep ordering in the deep pallial layers; axons navigating more superficially reached the SP of dorsolateral cortical zones, whereas those that extended more deeply in IZ or in SVZ invaded the SP of more medial cortical zones. As observed with DiI at the same ages, at the same point in which the axon contacted the SP, most primary growth cones had turned toward the cortical surface, and they were apparently beginning a radial advance into the overlying CP. The CP was still quite thin (50–100 μm) at this age, so a few cones even crossed the CP and reached the MZ (Marginal Zone, future layer I; Figs 3*C–F* and 7*A*). It is likely that these cones were subsequently either retracted, or overwhelmed by the rapid addition of new cell layers at the outer edge of the CP, because labeled growth cones were always confined to the CP for the following 4 days, and were only again seen to reach the MZ/layer I at postnatal ages (Fig. 7*A,C*). The labeled axons were generally smooth, although some already showed occasional short (<50 μm) branchlets always directed toward CP (Fig. 3*G*).

In the following days (E19–P0, Fig. 4), labeled axons slowly invaded the deep cortical layers. The intracortical portions of these axons were rather simple and mainly radial. They had few short (<100 μm) secondary branches that extended obliquely or tangentially in layer VI (Fig. 4*F*). In single 100-μm-thick sections these branches could systematically be traced to a tangentially oriented parent axon in SP or IZ that continued to more dorsomedially situated areas. In contrast, in the dorsomedial cortices, the invading axons apparently were the direct extension of primary growth cones.

The first Biocytin-labeled growth cones were observed inside layer I at P0 (Fig. 4*I,J*). Interestingly, these cones were always located in dorsomedial zones of the pallium, whereas growth cones in more lateral areas were still located at the bottom of CP, and were only found in layer I in significant numbers after P4.

Unfortunately, after P2, an area of ischemia systematically developed in the internal capsule in the tissue maintained "ex vivo." In the hemibrains, this point was the one located

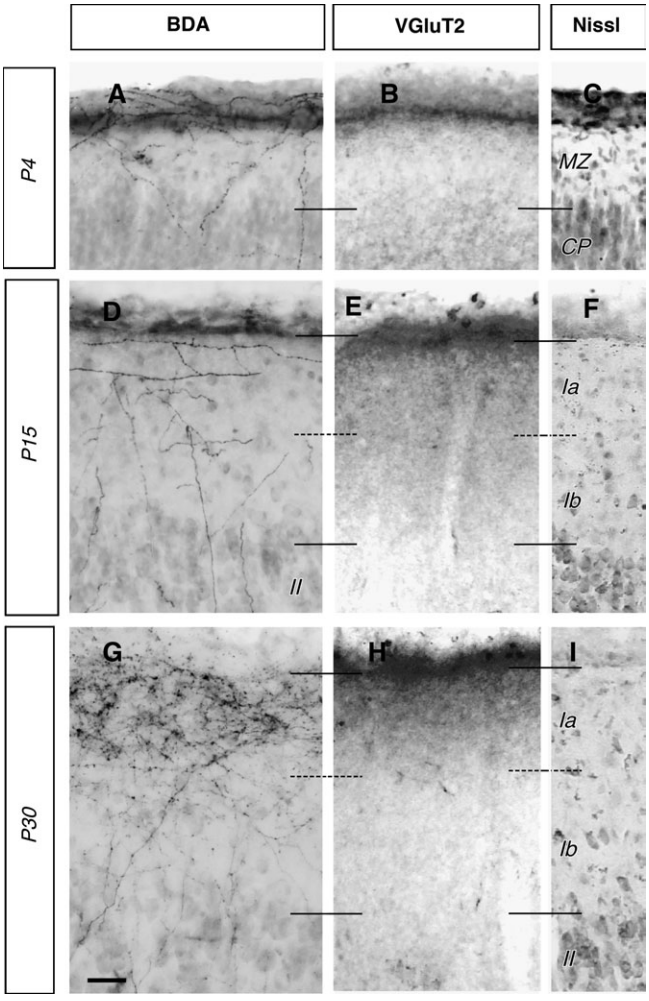


**Figure 6.** Sublamination of M-type axons in layer I during the postnatal period. The uppermost cortical layers and piamater of area M1 (motor cortex) are shown at 3 stages over the first postnatal month: P4 ("*A*"–"*C*"), P15 ("*D*"–"*E*"), and P30 ("*G*"–"*H*"). At each age, a field containing some BDA-labeled M-type axons after injections in Po (panels "*A*," "*D*," and "*G*") can be compared with parallel sections of an age-matched animal inmunostained for the VGluT2-ir (panels *B*, *E*, and *H*). Nissl-stained samples of the same region at each age are shown for reference (panels C,F,I). Bar = 25 μm.

furthest from any surface, suggesting that some critical distance for oxygen or nutrient diffusion was exceeded. This area interrupted the flow of Biocytin along the thalamocortical axons and rendered the "ex vivo" method unsuitable for rat brains aged P3 and older.

### *"In Vivo" Stereotaxic Microinjections of BDA in Postnatal Animals*

Iontophoretic microinjections of BDA were performed "in vivo" in P0–P30 animals in the Po or VM thalamic nuclei. Animals were allowed a minimum postinjection survival of 24 h before fixation; thus, the youngest age from which we obtained data with this technique was P1, after injections performed at P0. However, because of the small size of these nuclei and the lack of stable bone references in postnatal rats, we obtained comparable injection sites in only a limited number of cases. The series of comparable injections in Po was the most complete ($n$ = 21; Supplementary Material Fig. SM2); for this reason, the following account is essentially based on the observations in the Po experiments. Labeling after the few comparable injections in VM ($n$ = 5) generally resembled the pattern of labeling produced in layer I by Po injections, except for the noticeably fewer branches in layers V–III.

Injection sites produced by this technique were ~500–900 μm in diameter, although the labeling of local neuropil often gave the impression of a larger area. Axons labeled by Po injections were scattered throughout the parietal and dorsal frontal areas. Samples of labeling in the dorsal parietal cortex after Po injections are shown in Figure 5. Because of the relatively large number of axons labeled in these experiments, and the widespread areas that they reach, we could only examine their development mostly at the population level.

At P1, labeled Po axons were seen as axonal trunks running tangentially within IZ and SP. Collateral branches emerged perpendicularly from axon trunks under lateral parietal and rhinal areas and penetrated layers VI and V following radial or oblique trajectories; some showed additional secondary branches in these layers. In the dorsomedial areas the branches were longer; some of them had already extended their growth cone up to layer I (Fig. 8*G*).

**Figure 7.** Reconstructions and quantitation of the intracortical arbors of individual axons labeled "ex vivo" with Biocytin (E18–P0), or "in vivo" with BDA injections (P4–P6) in the Po nucleus. (*A*) Examples of axons reconstructed at 5 different ages are shown on a coronal brain section. For clarity, only a few axons per age are drawn. The reconstructed axons were preferentially selected from those showing clear labeling and complex arbors. Thus, the axon morphologies at each age might not proportionally represent the full spectrum of diversity. In the Figure, axons have been given different colors and considerably thickened to made them clearly visible. It must also be kept in mind that the reconstructed axon segments actually extended across many adjacent coronal sections. As a result, a total rostrocaudal extent of 500 (E18), 700 (E21), 800 (P0), 500 (P4), or 650 μm (P6) is "compressed" in each diagram. Arrowheads indicate the point at which each labeled thalamocortical axon entered the reconstructed volume from a more caudal level. Black dots at the medial end of some axons indicate the point that particular axon continued out of the reconstructed zone toward more frontal levels. It is to be underscored that although similar, the axons at different ages cannot be directly compared, because they correspond to different animals with injections in slightly different points of Po (See Supplementary Material Fig. SM1). As a result, the reconstructed frontoparietal cortex region in the "E21" or "P0" diagrams is more rostrally located than in the "P6" diagram. Observe the largely parallel arrangement of the axon trajectories in the deep pallial layers. Note the interstitial branches that many axons give off to innervate lateral cortical zones. Notice also that, in addition to the cortex, some of the branch into the striatum (diagrams P0, P4 and P6). Actual fragments of these extensive axon arbors, as seen in single coronal sections are shown in Figure 8. Str, striatum. Bar = 500 μm. For other abbreviations, see Figure 1. (*B*) Quantitative estimates of total axon length per intracortical arbor at different ages. Solid dots: axon arbors in dorsomedial cortex (prospective motor and cingulate areas); open circles: arbors in lateral cortex (prospective somatosensory and insular areas). Total number: 51 axons, minimum 5 axons per age group. (*C*) Quantitative estimate for leading growth-cone progression into the developing CP at the different ages. The position of the most superficial ("leading") cone of each axon arbor is represented as a percent of the total width from the inner edge of layer VI to the pial surface. In this representation, cortical width appears constant. Dots reflect a mean value for the population of axons reconstructed at each age. Note that fluctuations do not directly reflect the dynamic behavior of axons, but rather the changing net sum, in percentages, between the increase in radial axon length, against the expansion of cortical width due to the rapid insertion of new cell layers at the top of the CP. Conventions as in panel *B*.

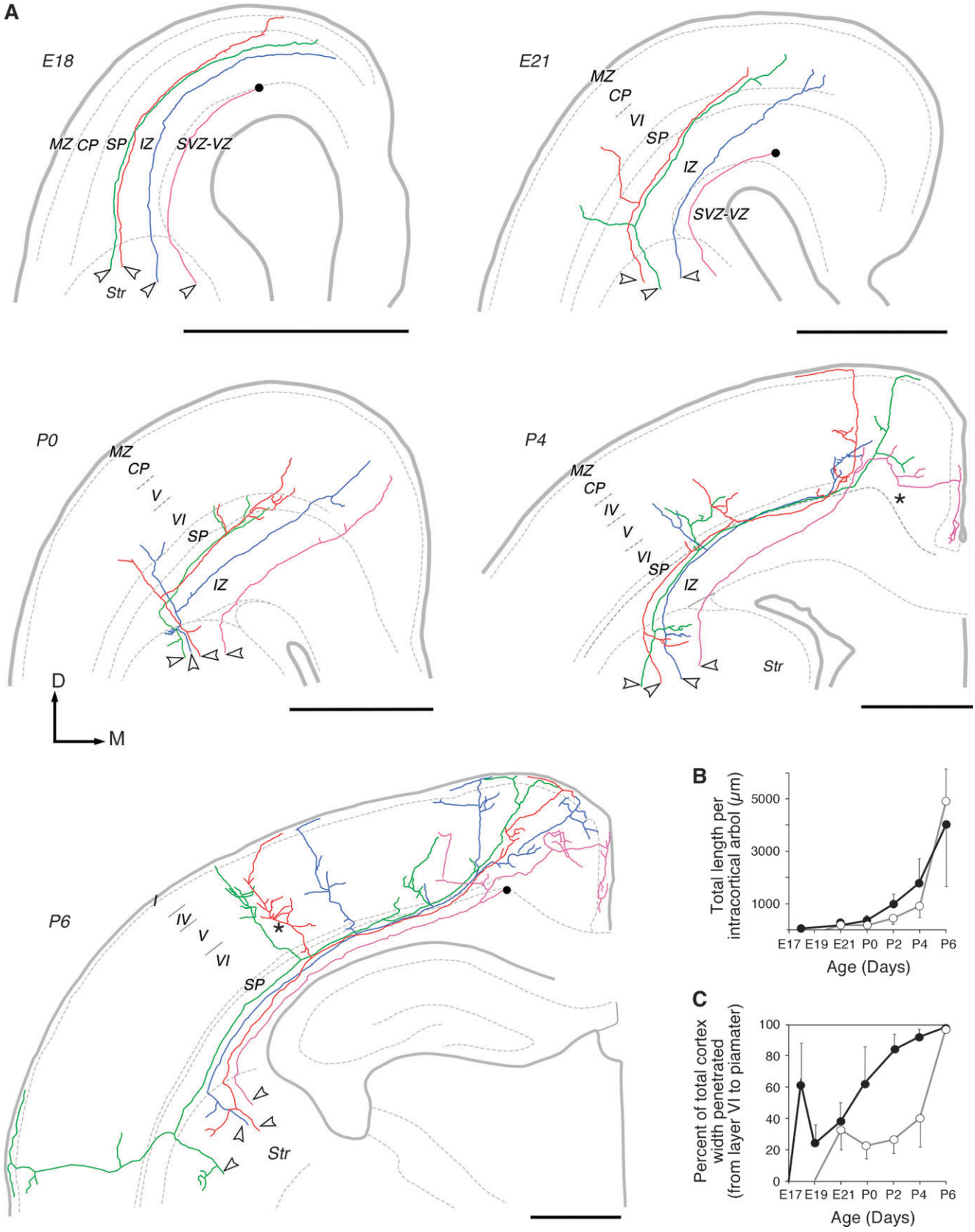
A
E18
MZ CP SP IZ SVZ-VZ
Str
E21
MZ
CP
VI
SP
IZ
SVZ-VZ
P0
MZ
CP
V
VI
SP
IZ
P4
MZ
CP
IV
V
VI
SP
IZ
Str
D
M
P6
I
IV
V
VI
SP
Str
B
Total length per intracortical arbol (μm)
5000
3000
1000
E17 E19 E21 P0 P2 P4 P6
Age (Days)
C
Percent of total cortex width penetrated (from layer VI to piamater)
100
80
60
40
20
0
E17 E19 E21 P0 P2 P4 P6
Age (Days)

Layer I triples in width over the first 2 postnatal weeks. During this period, M-type arbors in layer I increased their length, branching, and complexity (Fig. 6). Although the coronal sections were not well suited for addressing the branching pattern or length of tangential axon arbors in layer I, we nonetheless noticed some changes in the appearance and distribution of the labeled axon segments visible in single coronal sections. In the upper half of the layer (prospective sublayer Ia, Vogt 1991), most of these axon segments were tangentially oriented, and showed relatively few branching points. Numerous varicosities could be observed at high magnification. In contrast, in the lower half of the layer (future sublayer Ib), labeled axon segments were scant, and most had vertical or obliquely oriented trajectories. By the last age examined (P30) the relative abundance and laminar distribution of labeled M-type axon populations in the cortex (Fig. 6*G*) closely resembled that of the adult.

In addition to labeling of thalamocortical axons in layer I, it is to be noted that injections after P7 in Po labeled an increasingly dense horizontal plexus of profusely ramified axonal processes in the upper part of layer V in the parietal cortex (Fig. 5). Additional processes were labeled in the supragranular layers. Analysis of the correlation of these processes with the "barrels" in layer IV of the parietal cortex was beyond the scope of this study; however, it was evident that labeled axons extending across layer IV conspicuously avoided the periodically spaced domains of layer IV corresponding to the barrels. The same pattern was observed in Po injections made at P15 and P30.

### *Immunolabeling of the Thalamocortical Pathway with Antibodies against VGluT2*

As an indirect indicator of maturation by synapses from M-type axons during the first postnatal month in layer I, we examined the immunolabeling for VGluT2, a marker of functional presynaptic thalamocortical specializations (Fujiyama et al. 2001; Hur and Zaborszky 2005). The pattern of VGluT2 immunolabeling changed dramatically in this period (Fig. 6*B*, *E*, *H*). At P1, layer I immunolabeling was essentially at background levels (not shown). At P4, faint but above-background labeling was present in the most superficial zone of the layer. Two days later (P6), the intensity of the immunostaining in the superficial part of layer I had substantially increased. In the second and third postnatal weeks, the heavy labeling in the superficial half of layer I (sublayer Ia) rapidly reached the levels observed in adult rats (Fujiyama et al. 2001), with maximal density immediately under the piamater.

### *Reconstruction of Single M-type Axon Across Multiple Sections*

Single axons were reconstructed over multiple serial sections in experiments with small injections in comparable locations within Po made either "ex vivo" with biocytin (E18, E21, P0) or "in vivo" with BDA (P4, P6). Some injection sites are illustrated in Supplementary Material Figure SM1, whereas Figure 7 shows axons reconstructed at different ages. Details of the actual labeled axons are shown in Figure 8. The comparison between Figures 7 and 8 shows that these serial reconstructions are the only way to depict and detect the actual complexity of these very widespread axon arbors.

Overall, these experiments directly demonstrated that the primary growth cone of most axons first targeted a dorsomedial cortical zone. At later ages, axons gave off a few (1–2) interstitial branches directed to lateral cortical areas. By P4, the growth cones in the dorsomedial cortex had made a right angle turn in layer I extending tangentially under the piamater for up to several hundred microns (Figs 7 and 8*H*). Remarkably, at that time the growth cones on the branches of the same axons growing into lateral cortical areas were still in layer V. At P6, these axon branches in lateral areas had also reached layer I, and were extending tangentially under the pia. At the same age, subpial branches in the dorsomedial cortex had already given off some higher-order branches in layer I. In addition to arborization in layer I, single axon reconstructions revealed that various axon branches that penetrated the developing cortex also gave off higher-order branches in layers VI, V, and III by day P6. Our data regarding the late postnatal period (P15–P30) are limited to population level analysis (Fig. 5); nevertheless, comparison with adult Po arbors (Deschênes et al. 1998) suggests that these deeper branches eventually give rise to arbors in layers Va and III.

### *Retrograde Labeling of Thalamocortical Cells Targeting Layer I*

Because this invasion of cortical layer I, their primary target layer, is a key step in M-type axon development, we performed an independent set of experiments with retrograde tracing to confirm the timing of layer I invasion. The retrograde tracer FB was applied on the dura mater overlying the dorsal frontoparietal cortex immediately rostral to bregma (prospective M1 region) at different postnatal ages (Table 1). These deposits usually remained confined to the subpial zone of layer I; any experiments in which the tracer spread to the CP were discarded (Fig. 9*A*–*C*).

The results are summarized in Figure 9*D* and Supplementary Figure SM3. Epidural FB deposits at P0–P2 labeled only a few neurons scattered across thalamic nuclei such as the VM, ventrolateral, Po, and Reuniens. The scarcity of labeled thalamic neurons at P0–P2 was clearly not due to some problem in thalamic neuron ability for retrograde transport, because other experiments at the same ages produced large numbers of retrogradely labeled cells in the thalamus when the FB deposits extended more deeply into CP.

Retrogradely labeled cell somata in the thalamus became conspicuously more abundant after epidural deposits on P3 and later ages (Fig. 9D; Supplementary Fig. SM3). In these experiments, labeled neurons were most numerous in the VM, ventrolateral, and Po nuclei, with additional cells labeled in the mediodorsal, lateral posterior, and Reuniens nuclei. Deposits on P4 and P5 yielded similar distributions, and much the same or a slightly higher numbers of labeled cells.

### *Labeling of Collateral Axon Branches in the Striatum and Reticular Nucleus*

In addition to branches in the pallium, Biocytin and BDA labeling experiments revealed the branches that M-type axons give off to the reticular thalamic nucleus and striatum (Fig. 10*A*–*F*). In DiI experiments, these branching points were obscured by the large numbers of intense fluorescent labeled axons.

Between E17 and E21, no branches of thalamocortical axons were seen in subcortical structures. However, at E22, one or 2 small collateral branches could be seen on most of the labeled axons traversing the reticular thalamic nucleus. These branches

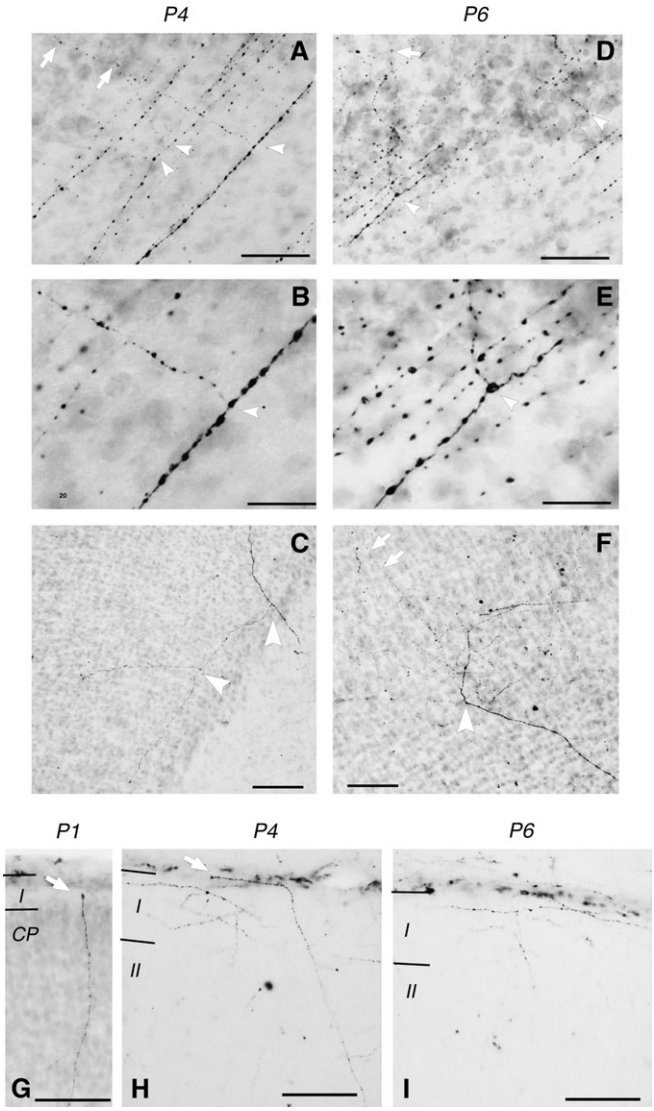


**Figure 8.** Photomicrographs of BDA-labeled axon fragments in postnatal animals as seen on single dry mounted sections that were100-μm thick at the time of tissue sectioning. (*A*, *C*) Labeled axons in the somatosensory cortex of P4 animals after Po injections. In panels "*A*" and "*B*" axon trunks can be seen running tangentially in SP, whereas perpendicular branches extend toward the pial surface, which lies toward the upper left corner of the image. Branching points are indicated by arrowheads. Panel "*C*" illustrates a fragment of a Po axon arbor in the deep layers of the motor cortex. The image corresponds to the portion of the *purple* axon indicated with an asterisk in the P4 diagram in Figure 7. (*D*–*F*) Axon segments labeled in the somatosensory cortex of P6 animals after injections in the Po nucleus. Panels "*C*" and "*D*" show branching points in the white matter, and panel "*F*" shows a fragment of a labeled arbor in layers VI and V of area S1. The latter corresponds to the region of the *red* axon indicated with an asterisk in diagram P6 in Figure 7. Note that a straight branch continues radially toward the pial surface (arrow). (*G*) The growth cone of a smooth, radially oriented axon sits at the border between the inner and outer half of layer I in a P1 case injected in VM. (*H*) A growth-cone tipped axon that shifted its elongation mode from radial to tangential in the outer half of layer I, and was now extending parallel to the pia, is shown in the motor cortex of a P4 animal injected in VM. Segments of other axons can be seen extending tangentially in the outer part of the layer. (*I*) A VM axon arborizing in layer I in a P6 animal after an injection in VM. The 2 morphologies exemplified in panels "*H*" and "*I*" are prevalent among M-type axons entering layer I. Observe that because of a "bevel" effect along the tissue border of these 50-μm-thick sections, a ribbon of piamater is superimposed onto the outer part of layer I in panels "*G*"–"*H*" (top). Some meningeal cells display nonspecific labeling. Bars: *A*, *C* = 50 μm; *B*, *D* = 25 μm; *E*–*I* = 100 μm. Abbreviations as in Figure 1.

emerged at right angles from the main axon trunk, and were markedly thinner than the trunk. By P0, branches in the reticular nucleus had become longer (up to 200 μm from the parent axon), and many had very small, but still recognizable, growth cones at their tips (Fig. 10*C*). In the following 2 days (P1–P2), the branches in the reticular thalamic nucleus continued to elongate, and started to grow smaller secondary ramifications (Fig. 7).

Beginning on E22, Biocytin injections in Po revealed interstitial branches extending into the striatum from the thalamocortical axons (Figs 7 and 10G). Likewise, most postnatal BDA injections in Po (P1–P30) labeled axon branches in the striatum. Thalamostriatal branches were not observed, however, after VM injections at any age.

## Discussion

The combined results from anterograde and retrograde labeling experiments revealed the timeline and main steps of M-type axon development from E16 to P30. These steps can be summarized as follows: 1) first, between E16 and E18, primary growth cones reach the SP of dorsally situated areas while the axons remain unbranched; 2) next, interstitial branches may sprout from the same axons under more lateral cortical regions, and invade the overlying cortex to become secondary arbors; 3) primary and secondary cones growing upwards across the cortical layers pause in the infragranular layers (E18–P0), and again in layer I (P0–P2); before 4) they begin subpial extension and arborization on P3–P4; finally 5) M-type axon arbors add evermore branches in sublayer Ia over the first postnatal month. Retrograde labeling experiments reveals that by P3–P4, large numbers of axons from multiple nuclei are already converging in a given spot of layer I. Our experiments also show that M-type axon branches to the striatum and reticular thalamic nucleus sprout 2–3 days after the cortical branches.

### *Trajectories and Targeting of Primary Growth Cones*

Between E16 and E18, M-type axons remained unbranched and basically parallel to each other on their way to the SP. The timing and subcortical trajectories of the M-type axons arising in Po or VM seem thus basically equivalent to those described for C-type neurons in other nuclei (Erzurumlu and Jhaveri 1990, 1992; Catalano et al. 1991; Molnár et al. 1998; López-Bendito and Molnár 2003), suggesting that both axon types may use similar guidance mechanisms for the initial stages of their navigation into the forebrain. These mechanisms are believed to involve membrane-bound and/or diffusible signals present in the subpallium (Braisted et al. 2000; Dufour et al. 2003; Seibt et al. 2003) and deep pallial layers (Bicknese et al. 1994; Gao et al. 1998; Mann et al. 2002; McQuillen et al. 2002; Uziel et al. 2002), as well as fasciculation with some early-developing axon systems previously extended between some of these structures (Metin and Godement 1996; Meyer et al. 1998; Molnár et al. 1998; Molnar and Cordery 1999).

### *Interstitial Branching of Thalamocortical Axons*

Axons from VM and Po neurons robustly innervate the lateral parietal and insular regions in the adult (Herkenham 1979, 1986; Deschênes et al. 1998; Monconduit and Villanueva 2005); thus, we were surprised to observe that the M-type axons labeled by our tracer deposits in these nuclei always extended their

primary growth cones to the dorsal and medial zones of the cerebral hemisphere. Examination of axons labeled at later ages revealed that the connections to lateral parietal and insular areas developed as secondary branches from axons whose primary cones had reached the dorsomedial cortex. The observation that branches appeared many hundreds of microns away from the primary growth cone 2–3 days after the cone had moved past the lateral cortex (Fig. 11) is consistent with the possibility that the branches are formed by the process known as interstitial sprouting (Szebenyi et al. 2001; Portera-Cailliau et al. 2005).

Several previous studies noted occasional collateral branches in thalamocortical axons under distant or "inappropriate" areas (Ghosh and Shatz 1992; Bicknese et al. 1994; Catalano et al 1996; Molnár et al. 1998), but regarded the branching to be transient. Because the above studies mainly examined nuclei where C-type neurons predominate, it is possible that most of the collateral branches that they observed were actually retracted (Bruce and Stein 1988; Naegele et al. 1988; Catalano et al. 1996; Krug et al. 1998). Moreover, because of the static nature of our preparations, it is even possible that events such as the elimination of some branches could have been underestimated by our study. In any case, taken together with single and double labeling axon tracing studies in the adult rat (Deschênes et al. 1998; Monconduit and Villanueva 2005), our data firmly indicate that some of the interstitial branches that sprout from Po and VM axons under lateral cortical areas are not transient, but grow to become full-grown intracortical arbors in the adult.

Interstitial axonal branching as a mechanism to reach multiple targets is common in some forebrain axon systems (O'Leary and Terashima 1988; Szebenyi et al. 2001), but had not been previously been considered in thalamocortical axons. The location at which interstitial sprouting occurs may depend on local signals acting on the primary growth cone at the time of its transit through the zone or on signals acting directly on the axon shaft (Szebenyi et al. 2003; Tang and Kalil 2005). Candidate signaling molecules include secreted or membrane-bound proteins such as LAMP (Mann et al. 1998), PSA-NCAM (Yamamoto et al. 2000), Netrin 1 (Dent et al. 2004), Anosmin 1 (Soussi-Yanicostas et al. 2002), or some growth factors and their receptors (Szebenyi et al. 2001; Yamamoto and Hanamura 2005).

### *Development of Branches to the Reticular Nucleus and Striatum*

Axon labeling after small thalamic Biocytin injections also revealed that about 3 days after branch sprouting from Po and VM axons had begun in the pallium on E18, additional collateral branches emerged from these axons in the reticular thalamic nucleus (Figs 9 and 11). The branches subsequently develop into thalamoreticular connections (Deschênes et al. 1998). These data accord with the observation in mice of a plexus of terminals in labeled VP axons in the reticular nucleus after P2, but not earlier (Agmon et al. 1995). If one considers that thalamocortical axons had been present in the reticular thalamic nucleus since E14, and that the reciprocal reticulothalamic connection invades the thalamus at E15 (Molnár et al. 1998), thalamoreticular collateral sprouting appears to be remarkably delayed.

In the case of Po axons, further collateral branches, which will eventually form thalamostriatal connections, begin to grow into the striatum at around E21. As far as we know, this is the first report on the timing of thalamostriatal pathway development. The collateral branches of Po axons that innervate the striatum (Deschênes et al. 1998) sprout at E21 from axons that had extended through this structure about a week earlier (E15; Catalano et al. 1991; Senft and Woolsey 1991; De Carlos and O'Leary 1992; Molnár et al. 1998). Again we find it remarkable that the thalamic axons had been in close vicinity with their target cells, in this case the striatal cells, for many days before the thalamostriatal branches sprouted. However, our data are limited to axons from Po and, it is thus possible that the thalamostriatal connections from other thalamic nuclei (Erro et al. 2002) develop at different ages.

### *Invasion and Layer-Specific Arborization of M-Type Axons*

In contrast to the swift tangential navigation of primary growth cones from the thalamus to their target SP areas, the subsequent radial invasion of layer I requires almost a week (E18–P2; Fig. 12). A slower progression across the infragranular layers was also noted in C-type axons, and interpreted to reflect an active process of sorting and local remodeling that would contribute to the observed rearrangements within the subcortical white matter and deep cortical layers that refine the intra-areal topography of thalamocortical axons in supragranular layers (Agmon et al. 1993; Adams et al. 1997; Catalano and Shatz 1998; López-Bendito and Molnár 2003; Shimogori and Grove 2005). In this process, extension, retraction, and/or branching are believed to depend on interactions with secreted or membrane-bound signals present in the deep cortical layers (López-Bendito and Molnár 2003), as well as on activity-dependent mechanisms that may be mediated by early, transient synaptic contacts (Friauf and Shatz 1991; Hanganu et al. 2002; Higashi et al. 2005).

**Figure 9.** Timing of axon arborization into the superficial tier of layer I (sub layer Ia) as revealed by means of epidural deposits of the retrograde tracer FB. (*A*) Diagram of the experimental design. A small piece of thin paper FB-soaked was surgically placed onto the intact dura mater of the dorsal frontoparietal cortex. The location of the placement on a diagrammatic dorsal view of a postnatal rat brain is shown in the inset. The paper pushed the dura mater against the piamater, and, as a result, FB impregnated both meninges and a fraction of the tracer permeated into the upper region of the underlying layer I. After 24–48 h survival, numerous neuronal somata were labeled in a tissue "column" under the deposit. (*B*, *C*) Coronal sections across the center of cortical zones impregnated by an epidural deposit in a P2 ("*B*") and P3 animal ("*C*"). The dura and FB-soaked paper were removed prior to sectioning. Because of the intense glow of the adjacent piamater (PM), fluorescence in layer I appears relatively low at this magnification; however, the superficial part of this layer (future sub layer Ia) was impregnated by FB and fluorochrome uptake took place only from it. Large numbers of tightly packed neuronal somata are labeled in some of the underlying cortical layers. These cells probably captured the tracer through an apical dendrite that reached into layer I, because somata are labeled only in layers V and II–III, whereas layer VI and SP, which do not have cells with dendrites that reach layer I, remained unlabeled. (*D*) Diagrammatic drawings of the retrograde neuronal labeling present in the ipsilateral thalamus after 4 epidural deposit experiments performed at different postnatal ages. Labeled neurons (black dots, each dot represents one neuron) are shown on representative serial coronal sections taken at roughly equivalent coronal levels from P1, P2, P3, and P4 experiments (4 sections per case). All animals received an epidural FB deposit in virtually identical points of the dorsal frontoparietal cortex near the bregma (inset in panel "*A*"). Tracer impregnation was always confined to the upper MZ. Observe that the number of neurons increases rather abruptly between P2 and P3. Abbreviations: IAM, interanteromedial nucleus; Re, reunions nucleus; VA, ventral anterior nucleus; VP, ventroposterior complex; LD, laterodorsal nucleus; VL, ventrolateral nucleus; Eth: ethmoid nucleus; Pc, paracentral nucleus; MD, mediodorsal nucleus; Pf, parafascicular nucleus. Other abbreviations, as in Figure 1. Bars *B*, *C* = 200 μm; *D* = 1 mm.

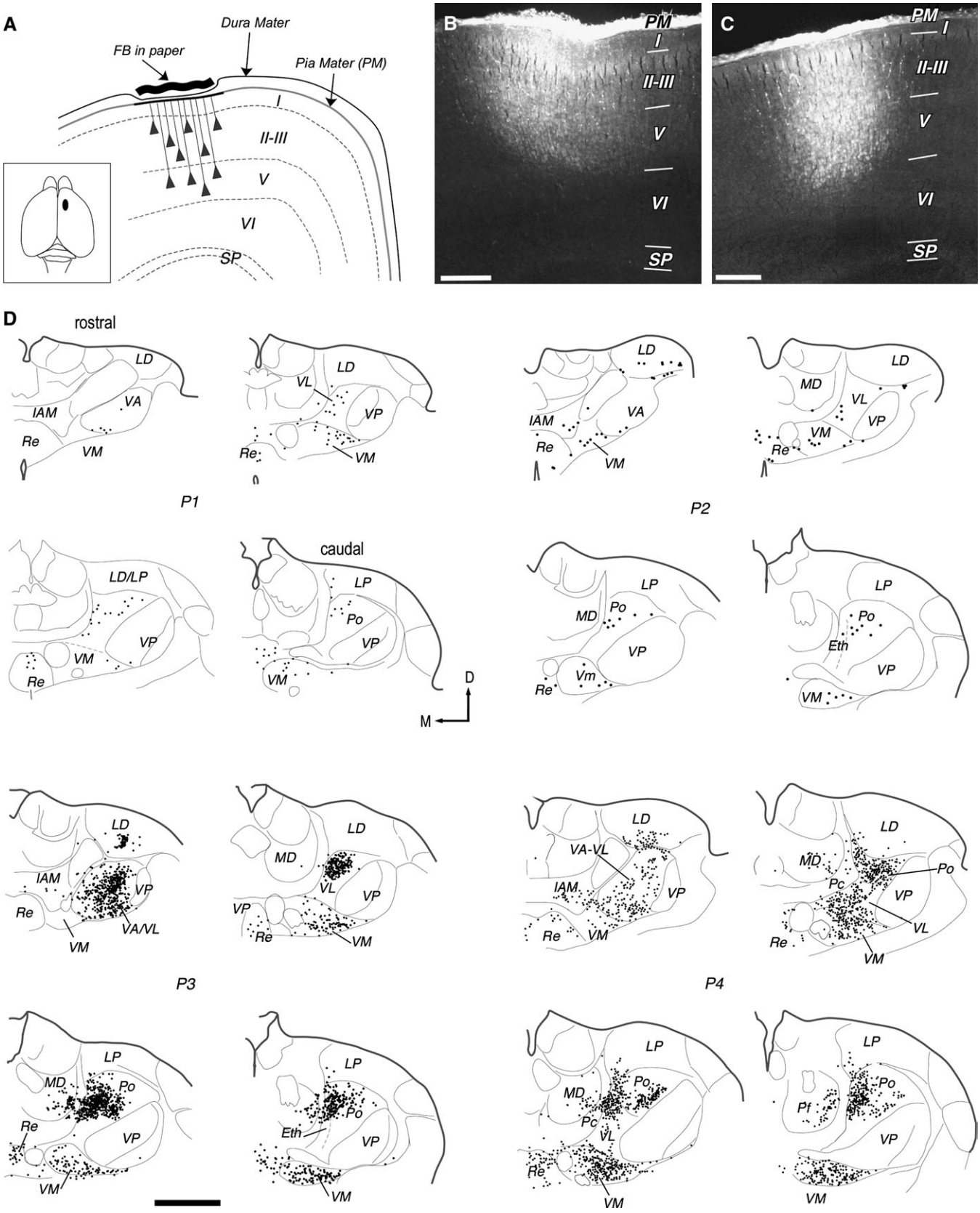
A
Dura Mater
FB in paper
Pia Mater (PM)
I
II-III
V
VI
SP
B
PM
I
II-III
V
VI
SP
C
PM
I
II-III
V
VI
SP
D
rostral
LD
IAM
VA
Re
VM
VL
VP
MD
LD/LP
caudal
LP
Po
Vm
Eth
Pf
VA/VL
VA-VL
Pc
P1
P2
P3
P4
D
M

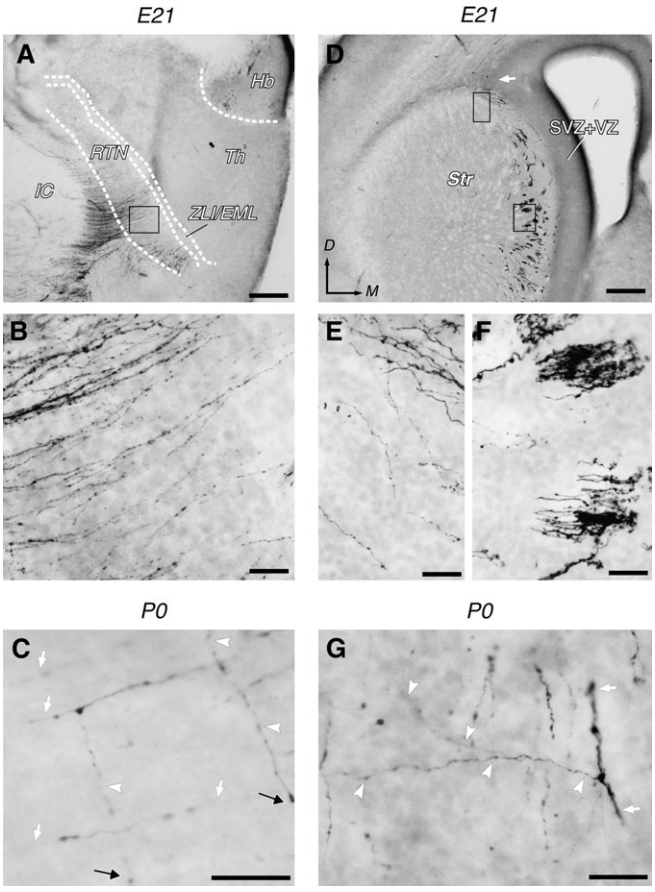


**Figure 10.** Development of thalamoreticular and thalamostriatal branches from Po nucleus M-type axons. (*A*) Axons labeled after an injection in the Po nucleus at E21 can be seen traversing the reticular nucleus (RTN) and entering the internal capsule (IC). (*B*) High-magnification view of labeled thalamocortical axons in the reticular nucleus at E21 (inset in "*A*"). Note that axons show no branches. (*C*) High-magnification detail of labeled thalamocortical axons in the reticular nucleus at P0. The image corresponds to a field equivalent to that in panel "*B*," and has the same orientation. Interstitial branches (indicated by white arrowheads) can be seen extending perpendicularly from the main trunks of thalamocortical axons (also indicated by white arrows). Note that the branches are capped by growth cones (black arrows), which grow parallel to the main axis of the RTN. (*D*) Labeled axons traversing the mantle layer of the developing striatum (Str) in the same experiment. Note that the axons are widely dispersed in numerous small fiber bundles. At the level of the striato-pallial border (arrow), some axons can be seen extending into the pallial layers. (*E*, *F*) High-magnification views of labeled axons in the striatal mantle layer. Note that at his age, axons do not yet show collateral branches in the striatum. (*G*) High-magnification view of labeled axons in the striatum at P0. An interstitial branch can be seen extending from a thicker parent axon trunk (indicated by arrowheads). Observe that the branch is itself divided into 2 braches that extend toward lateral zones of the striatum. Other abbreviations: Hb, habenula; ST, stria terminalis; ZLI/EML, zonal limitans intrathalamica/external medullary lamina; Th, dorsal thalamus. Bars *A*, *D* = 250 μm; *B*, *E*, *F*, *G* = 25 μm; *C* = 20 μm.

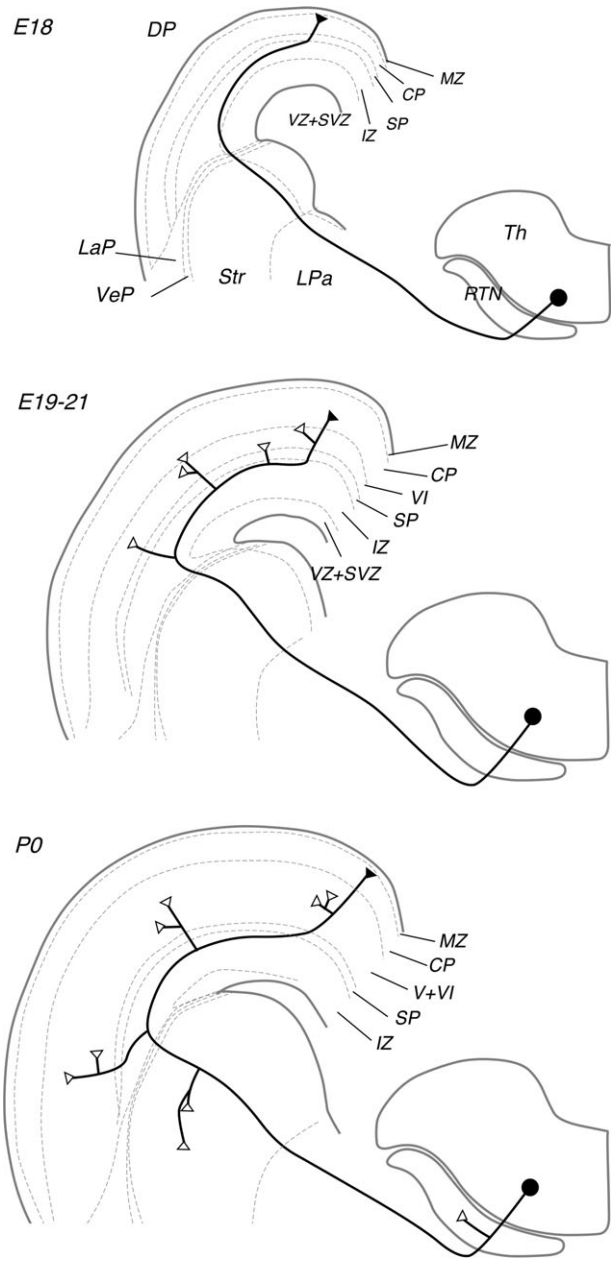


**Figure 11.** Schematic summary of the sequence of M-type axon branching in the cerebral cortex (dorsal pallium, DP), striatum (Str) and reticular thalamic nucleus. Three stages (E18, E19–21, and P0) are displayed from top to bottom. In each stage, an idealized M-type axon is shown extending away from the thalamus and successively traversing the reticular thalamic nucleus (RTN), lateral pallidum (LPa), Str, and the pallio-subpallial border, which contains the deep portions of radial glia cells of the lateral pallium (LaP) and ventral pallium (VeP). By E18 (diagram at the top), the distal growth cone (black triangle) has already reached the SP layer of the DP (prospective neocortex). Between E19 and E21, (diagram at the center) the axon develops first-order branches, both near the distal growth cone and more proximally, under the lateral parts of DP. By P0 (diagram at the bottom), some of these branches are developing into complex intracortical arbors. In contrast with the early emergence of branches in the pallial segment of the axons, collateral branches to Str and RTN develop later, around P0. Other abbreviations as in Figure 1.

M-type axon development has not been specifically examined with in vitro assay techniques. However, cocultures of rat thalamus (presumably including both C-type and M-type cells) and cortical explants taken at different ages have shown that thalamic axons extend en masse across the CP out to MZ on E19–P1 cortical explants (Yamamoto et al. 1997; Molnár and Blakemore 1999; Poskanzer et al. 2003). In cortical explants taken from P2 and older animals, however, some "stop" signals appear in the middle layers of the explants, that halt C-type growth cones. Remarkably, this arrest apparently does not interfere with the extension of at least some M-type axons to the marginal zone (Yamamoto et al. 1997). Moreover, C-type axons can be reverted to their early in vitro behavior of extension into layer I in cortical explants older than P2 by the application of antibodies or blocking peptides against N-cadherin (Poskanzer et al. 2003). Comparison of these in vitro

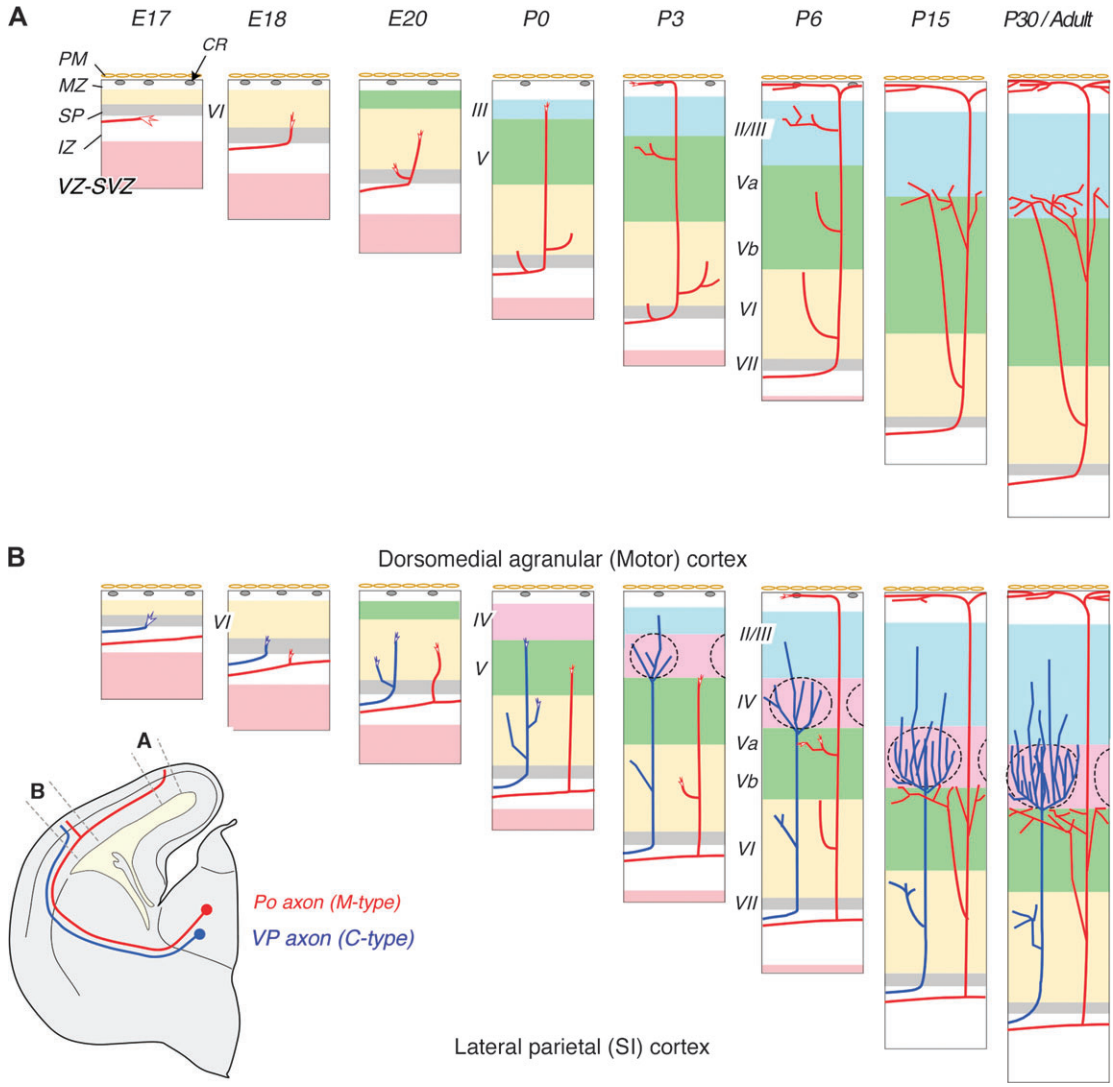


**Figure 12.** Highly schematic interpretation of the temporal sequence for lamina-specific invasion and arborization of thalamocortical M-type axons in dorsomedial or lateral zones of the cortex. Idealized columnar "samples" from the dorsomedial agranular cortex (*A*) and lateral parietal cortex (*B*) are represented at different ages, as indicated. In the samples, the pial surface is at the top and the ventricular surface at the bottom. In each sample, the approximate relative widths of the cellular layers of the pallium are indicated by different colors. The dense CP is not identified as such in this figure; instead, the colors represent the developing cortical layers as inferred from neurogenesis studies in rats (Bayer and Altman 1991; Catalano et al. 1996). Note the rapid insertion of new cell layers at the lower border of the marginal zone (MZ) during the prenatal period. Note also the expansion or disappearance of some layers in the postnatal period. The piamater (PM) is represented as a row of planar brown cells. For reference Cajal-Retzius cells (CR) are also depicted; these transient cells coexist for about a week with M-type axons in layer I (Meyer et al. 1998; Portera-Cailliau et al. 2005). On the upper row of cortical samples ("*A*"), an idealized M-type Po nucleus axon targeting a dorsal cortical zone is represented (red line). In the lower row ("*B*"), a collateral branch from the same axon targeting a lateral cortical zone is shown likewise. Compare with the figurine on the left for orientation on the trajectory of this axon. The "adult" arbor pattern of this axon is based on reports by others (Deschênes et al. 1998). In addition, for comparison, an idealized C-type axon from the ventroposterior (VP) nucleus (blue line) is represented in "*B*." This VP axon targets a single barrel in area SI. The developmental sequence of the VP axon is derived from published studies (Jensen and Killackey 1987; Catalano et al. 1996). Dashed line circles represent "barrel" domains in layer IV. Note that invasion of layer I by the Po axon occurs in SI after P3, whereas the same M-axon invades the dorsal frontal cortex layer I some days earlier (P0–P1). Observe that in SI (row "*B*") the Po axon also arborizes in layer Va, whereas the VP axon arborizes in layer VI instead. For other abbreviations, see Figure 1.

results with DiI observations in E19–P2 brains suggests that extension across the supragranular layers by both C-type and M-type axons is prevented by signals that are present in the upper cortical layers in vivo, but are apparently absent in coculture assays. Alternatively, interactions between thalamic axons and intermediate subcortical targets (Garel and Rubenstein 2004; Vanderhaeghen and Polleux 2004) might modify the default response by the thalamic axons to CP cues, and, again, this cannot happen in cocultures.

Present data indicate that layer I is innervated by M-type axons in 2 successive steps (Fig. 12). First (E22–P2), radial processes cross the dense CP and reach the inner part of layer I (sublayer Ib) without branching. For about 2 days, the growth cones of these processes seemingly "wait" at some distance from the pia (Figs 2, 3*I,J*, and 6*G*). Finally, at about P2–P3, the cones abruptly turn and begin their tangential extension into the upper part of layer I, right under the piamater (Figs 6*A*, 7, and 8*H*). After P4, some higher-order branches sprout from these subpial processes.

Reconstruction of single axons innervating different cortical areas also shows that, in the first postnatal days, axon arbor development is about 2 days more advanced in the dorsomedial cortex, which is innervated by the primary growth cone, than in the lateral cortex, which is targeted by collateral branches

(Figs 7*A* and 12). For C-type axons, the timing of layer-specific invasion is finely regulated by factors intrinsic to the CP (Shimogori and Grove 2005; Yamamoto and Hanamura 2005). Hence, it is possible that the advanced development of M-type primary arbors in the dorsomedial cortex reflects an earlier maturation of guidance signaling in dorsomedial cortex. This early arborization contrasts with the delayed neurogenesis and layer differentiation in the dorsomedial cortex (Bayer and Altman 1991; Meyer et al. 1998) and raises the possibility that primary and secondary cones of M-type axons might react differently to cortical signals.

Tangential extension within sublayer Ia represents the terminal arborization phase of M-type axons. The observed delay between initial radial growth and tangential extension along layer I would thus be in register with observations of thalamocortical C-type axons that layer-specific targeting and arborization are different processes (Yamamoto et al. 2000; Mann et al. 2002). Molecular signals regulating each process (reviewed in Yamamoto and Hanamura 2005) may be to some extent different for M-type and C-type axons. Moreover, the conspicuous "flattening" and extensive tangential elongation of M-type axon arbors within sublayer Ia begs for the existence of some source of patterning signals in the cortical surface; potential candidates include Cajal-Retzius neurons (Meyer et al. 1998; Portera-Cailliau et al. 2005) and piamater cells (Borrell and Marin 2006).

In addition to arborization in layer I, higher-order branches were seen sprouting from some Po axons in layer Va and, less frequently, also in layer III (Figs 7, 11, and 12). Subsequently, these deep branches arborized profusely (Figs 5, 7, and 12). These arborizations are also found in adult rats (Herkenham 1986; Lu and Lin 1993; Deschênes et al. 1998). In contrast, in our material, branches in VM arbors in layers V–II were simpler and much scarcer, consistent with the observations in adult rats that VM axons scarcely innervate these layers (Herkenham 1979; Arbuthnott et al. 1990).

### *Postnatal Sublayering of M-Type Axon Arbors in Layer I*

Between P0 and P15, the width of layer I increases about 3-fold (Ichinohe et al. 2003) and the sublayering found in adults becomes progressively more evident (Vogt 1991; Ichinohe and Rockland 2004). Our coronal sections were not suited for visualizing the large subpial axon arbors from M-type cells (Ferster and LeVay 1978; Portera-Cailliau et al. 2005); nevertheless, we could observe the morphology of axon segments contained in single sections (Figs 5, 6, and 12). Most segments were situated in sublayer Ia, had tangential trajectories, and showed numerous varicosities. The varicosities probably correspond to developing "en passant" synaptic boutons, as in adult M-type axons (Arbuthnott et al. 1990; Lu and Lin 1993). In some branches, however, they might also reflect regressive changes occurring after birth in these axons (Portera-Cailliau et al. 2005).

A parallel assessment of changes in the immunolabeling for VGluT2, a marker of presynaptic thalamic specializations (Fujiyama et al. 2001; Hur and Zaborszky 2005), revealed a steady increase and restriction to sublayer Ia during the first postnatal month. This is in consonance with reports of robust synaptic activity in layer I evoked by thalamic stimulation in brain slices from postnatal mice (Llinás et al. 2002), as well as with observations in laminar field potential analysis studies after thalamic stimulation in postnatal kittens (Kato et al. 1983; Kato 1987).

### *Convergence of Axons in Layer I*

To determine the overall population of thalamocortical cells with axons that had reached layer I at each postnatal day, we made FB deposits limited to layer I (Fig. 9A-C). Two observations suggest that effective tracer uptake occurred only at or near the subpial surface of this layer. First, the FB deposits on the lateral parietal cortex (data not shown) between P0 and P5 never produced labeling in neurons in the ventroposterior nucleus, from which axons may occasionally extend up to the inner tier of the marginal zone at these ages (Erzurumlu and Jhaveri 1990; Catalano et al. 1996). Second, comparison of the results of retrograde labeling in the thalamus with those of anterograde labeling in the cortex over the same time course shows that labeling of large numbers of neurons in the thalamus coincides with the beginning of tangential subpial extension of axons in layer I at P3, rather than with their initial entry into the deep part of this layer at P0. Importantly, lack of thalamic labeling at P0–P2 was not due to immaturity of axon transport mechanisms, because deposits that extended into the deep cortical layers at the same ages labeled many thalamic neurons.

Our retrograde FB data reveal that a massive number of axons from different thalamic nuclei are beginning to arborize subpially by P3 in the dorsal frontal cortex (presumptive motor area). Comparison with equivalent FB deposits in the adult rat (Mitchell and Cauller 2001; Rubio-Garrido et al. 2004) shows that these connections are not transient. Targeting errors in axon arbors reaching layer I thus seem to be minimal. Studies in different species with retrograde tracer injections involving the whole width of the cortex have reported postnatal elimination of some initially exuberant or "inappropriate" thalamic connections (Bruce and Stein 1988; Naegele et al. 1988; Darian-Smith C and Darian-Smith I 1993; Krug et al. 1998). It is to be noted, however, that such exuberant connections apparently depended on collateral branches that never extended into the upper cortical layers (Naegele et al. 1988; Ghosh and Shatz 1992; López-Bendito and Molnár 2003), unlike the arborizations of M-type axons in layer I described in the present study.

Present data show that a large and diverse group of M-type thalamocortical axons converge in any given domain of layer I in the first postnatal days, creating the possibility of early interactions in layer I. Interactions between M-type axons, the developing pryramidal cell apical dendrites, local interneurons (Meyer et al. 1998), and other early-arriving afferents systems such as serotonergic axons (Janusonis et al. 2004) may be thus be extensive, and highly significant for the assembly of cortical microcircuits.

### *Dissociation between M-Type and C-Type Axons in the Timing of their Layer-Specific Targeting*

Our observations after FB deposits in the motor cortex show that, in this dorsomedially situated area, virtually all the M-type axons that will innervate layer I in the adult invade this layer almost simultaneously around P3.

However, our anterograde tracing data also suggest that, in other areas, layer I invasion by M-type axons originated in different thalamic nuclei may occur at different times. For example, we show here that some Po axons innervating the primary somatosensory (SI) cortex arborize in layer I around P5 (Figs 7 and 12*B*), whereas other rat studies have shown that the C-type axons from the ventroposterior nucleus arborize in SI layer IV at P2 (Erzurumlu and Jhaveri 1990, 1992; Catalano et al.

1991, 1996). Similarly, an early study using horseradish peroxidase microinjections in layer I of rat visual cortex reported retrograde labeling in the lateral posterior nucleus at younger ages than in the dorsal lateral geniculate nucleus (Parnavelas and Chatzissavidou 1981). In addition, some studies in mammals with protracted cortical development such as primates (Rakic 1977), carnivores (Kato et al. 1983, 1986; Lushkin and Shatz 1986; Ghosh and Shatz 1992; Noctor et al. 2001), or marsupials (Sheng et al. 1991; Marotte et al. 1997) noted broad differences between the timing first appearance of anterograde thalamocortical labeling in layers I or IV.

In sum, the present study in rats shows that although the initial extension of M-type axons into the pallium is basically comparable with that reported for C-type axons, the mechanisms for area targeting, invasion, and layer-specific arborization are markedly different in each axon type. These developmental differences underscore the phenotypic divide between M-type and C-type thalamocortical neurons. Moreover, the study reveals that, as a result of their early ingrowth into layer I in large numbers, M-type axons are in position to significantly influence the early development of cortical circuits.

## Supplementary Material

Supplementary material can be found at http://www.cercor.oxfordjournals.org/.

## Notes

The authors wish to thank Dr Carlos Avendaño for critical reading of a previous version of the manuscript, Carol F. Warren for linguistic assistance, and Jorge Castro for help with the Neurolucida software.

Support: Grants from Spanish Ministry of Education & Science Grants BFU-BFI 2002-04674 and 2005-07857, Comunidad de Madrid 08.5/0002.1/2001 and Fundación Eugenio Rodriguez Pascual. M.J.G. is supported by a FPU-MEC fellowship; C.P.C. is supported by a FPU-UAM fellowship. *Conflict of Interest*: None declared.

Address correspondence to Dr Francisco Clascá, Department of Anatomy & Neuroscience, School of Medicine, Autónoma University, Ave. Arzobispo Morcillo s/n., Madrid, Spain E-28029. Email: francisco.clasca@uam.es.

## References

Adams NC, Lozsadi DA, Guillery RW. 1997. Complexities in the thalamocortical and corticothalamic pathways. Eur J Neurosci. 9:204–209.

Agmon A, Yang LT, Jones EG, O'Dowd DK. 1995. Topological precision in the thalamic projection to neonatal mouse barrel cortex. J Neurosci. 15:549–561.

Agmon A, Yang LT, O'Dowd DK, Jones EG. 1993. Organized growth of thalamocortical axons from the deep tier of terminations into layer IV of developing mouse barrel cortex. J Neurosci. 13:5365–5382.

Arbuthnott GW, MacLeod NK, Maxwell DJ, Wright AK. 1990. Distribution and synaptic contacts of the cortical terminals arising from neurons in the rat ventromedial thalamic nucleus. Neuroscience. 38:47–60.

Auladell C, Perez-Sust P, Supèr H, Soriano E. 2000. The early development of thalamocortical and corticothalamic projections in the mouse. Anat Embryol. 201:169–179.

Avendaño C, Rausell E, Reinoso-Suarez F. 1985. Thalamic projections to areas 5a and 5b of the parietal cortex in the cat: a retrograde horseradish peroxidase study. J Neurosci. 5:1446–1470.

Avendaño C, Stepniewska I, Rausell E, Reinoso-Suarez F. 1990. Segregation and heterogeneity of thalamic cell populations projecting to superficial layers of posterior parietal cortex: a retrograde tracer study in cat and monkey. Neuroscience. 39:547–659.

Bayer SA, Altman J. 1991. Neocortical development. New York: Raven.

Bernardo KL, Woolsey TA. 1987. Axonal trajectories between mouse somatosensory thalamus and cortex. J Comp Neurol. 258:542–564.

Bicknese AR, Sheppard AM, O'Leary DD, Pearlman AL. 1994. Thalamocortical axons extend along a chondroitin sulfate proteoglycan-enriched pathway coincident with the neocortical subplate and distinct from the efferent path. J Neurosci. 14:3500–3510.

Borrell V, Marin O. 2006. Meninges control tangential migration of hem-derived Cajal-Retzius cells via CXCL12/CXCR4 signaling. Nat Neurosci. 9:1284–1293.

Boyd JD, Matsubara JA. 1996. Laminar and columnar patterns of geniculocortical projections in the cat: relationship to cytochrome oxidase. J Comp Neurol. 365:659–682.

Braisted JE, Catalano, SM, Stimac R, Kenendy TE, Tessier-Lavigne M, Shatz CJ, O'Leary DDM. 2000. Netrin-1 promotes thalamic axon growth and is required for proper development of the thalamocortical projection. J Neurosci. 20:5792–5801.

Bruce LL, Stein BE. 1988. Transient projections from the lateral geniculate to the posteromedial lateral suprasylvian visual cortex in kittens. J Comp Neurol. 278:287–302.

Carey RG, Fitzpatrick D, Diamond IT. 1979. Layer I of striate cortex of Tupaia glis and Galago senegalensis: projections from thalamus and claustrum revealed by retrograde transport of horseradish peroxidase. J Comp Neurol. 186:393–437.

Castro-Alamancos MA, Connors BW. 1997. Thalamocortical synapses. Prog Neurobiol. 51:581–606.

Catalano SM, Robertson RT, Killackey HP. 1991. Early ingrowth of thalamocortical afferents to the neocortex of the prenatal rat. Proc Natl Acad Sci USA. 88:2999–3003.

Catalano SM, Robertson RT, Killackey HP. 1996. Individual axon morphology and thalamocortical topography in developing rat somatosensory cortex. J Comp Neurol. 367:36–53.

Catalano SM, Shatz CJ. 1998. Activity-dependent cortical target selection by thalamic axons. Science. 281:559–562.

Cauller L. 1995. Layer I of primary sensory neocortex: where top-down converges upon bottom-up. Behav Brain Res. 71:163–170.

Chang SL, LoTurco JJ, Nisenbaum LK. 2000. In vitro biocytin injection into perinatal mouse brain: a method for tract tracing in developing tissue. J Neurosci Methods. 97:1–6.

Clancy B, Cauller LJ. 1999. Widespread projections from subgriseal neurons (layer VII) to layer I in adult rat cortex. J Comp Neurol. 407:275–286.

Condè F, Audinat E, Maire-Lepoivre E, Crepel F. 1990. Afferent connections of the medial frontal cortex of the rat. A study using retrograde transport of fluorescent dyes. I. Thalamic afferents. Brain Res Bull. 24:341–354.

Cruikshank SJ, Killackey HP, Metherate R. 1991. Parvalbumin and calbindin are differentially distributed within primary and secondary subregions of the mouse auditory forebrain. Neuroscience. 105:553–569.

Darian-Smith C, Darian-Smith I. 1993. Thalamic projections to areas 3a, 3b, and 4 in the sensorimotor cortex of the mature and infant macaque monkey. J Comp Neurol. 335:173–199.

Deacon TW, Eichenbaum H, Rosenberg P, Eckmann KW. 1983. Afferent connections of the perirhinal cortex in the rat. J Comp Neurol. 220:168–190.

De Carlos JA, O'Leary DDM. 1992. Growth and targeting of subplate axons and establishment of major cortical pathways. J Neurosci. 12:1194–1211.

Dent EW, Barnes AM, Tang F, Kalil K. 2004. Netrin-1 and semaphorin 3A promote or inhibit cortical axon branching, respectively, by reorganization of the cytoskeleton. J Neurosci. 24:3002–3012.

Desbois C, Villanueva L. 2001. The organization of lateral ventromedial thalamic connections in the rat: a link for the distribution of nociceptive signals to widespread cortical regions. Neuroscience. 102:885–898.

Deschênes M, Veinante P, Zhang ZW. 1998. The organization of corticothalamic projections: reciprocity versus parity. Brain Res Brain Res Rev. 28:286–308.

Dufour A, Seibt J, Passante L, Depaepe V, Ciossek T, Frisen J, Kullander K, Flanagan JG, Polleux F, Vanderhaeghen P. 2003. Area specificity and

topography of thalamocortical projections are controlled by ephrin Eph genes. Neuron. 39:453–465.
Erro ME, Lanciego JL, Giménez-Amaya JM. 2002. Re-examination of the thalamostriatal projections in the rat with retrograde tracers. Neurosci Res. 42:45–55.
Erzurumlu RS, Jhaveri S. 1990. Thalamic axons confer a blueprint of the sensory periphery onto the developing rat somatosensory cortex. Brain Res Dev Brain Res. 56:229–234.
Erzurumlu RS, Jhaveri S. 1992. Emergence of connectivity in the embryonic rat parietal cortex. Cereb Cortex. 2:336–352.
Ferster D, LeVay S. 1978. The axonal arborizations of lateral geniculate neurons in the striate cortex of the cat. J Comp Neurol. 182:923–944.
Foster GA. 1998. Chemical neuroanatomy of the prenatal rat brain. A developmental atlas. Oxford: Oxford University Press.
Friauf E, Shatz CJ. 1991. Changing patterns of synaptic input to subplate and cortical plate. J Neurophysiol. 66:2059–2071.
Fujiyama F, Furuta T, Kaneko T. 2001. Immunocytochemical localization of candidates for vesicular glutamate transporters in the rat cerebral cortex. J Comp Neurol. 435:379–387.
Gao PP, Yue Y, Zhang JH, Cerretti DP, Levitt P, Zhou R. 1998. Regulation of thalamic neurite outgrowth by the Eph ligand ephrin-A5: implications in the development of thalamocortical projections. Proc Natl Acad Sci USA. 95:5329–5334.
Garel S, Rubenstein JL. 2004. Intermediate targets in formation of topographic projections: inputs from the thalamocortical system. Trends Neurosci. 27:533–539.
Garraghty PE, Sur M. 1990. Morphology of single intracellularly stained axons terminating in area 3b of macaque monkeys. J Comp Neurol. 294:583–593.
Ghosh A, Shatz CJ. 1992. Pathfinding and target selection by developing geniculocortical axons. J Neurosci. 12:39–55.
Halloran MC, Kalil K. 1994. Dynamic behaviors of growth cones extending in the corpus callosum of living cortical brain slices observed with video microscopy. J Neurosci. 14:2161–2177.
Hanganu IL, Kilb W, Luhmann HJ. 2002. Functional synaptic projections onto subplate neurons in neonatal rat somatosensory cortex. J Neurosci. 22:7165–7176.
Hashikawa T, Rausell E, Molinari M, Jones EG. 1991. Parvalbumin- and calbindin-containing neurons in the monkey medial geniculate complex: differential distribution and cortical layer specific projections. Brain Res. 544:335–341.
Herkenham M. 1979. The afferent and efferent connections of the ventromedial thalamic nucleus in the rat. J Comp Neurol. 183:487–517.
Herkenham M. 1986. New perspectives on the organization and evolution of nonspecific thalamocortical projections. In: Jones EG, Peters A, editors. Cerebral cortex. Vol. 5. New York: Plenum. p. 403–445.
Higashi S, Hioki K, Kurotani T, Kasim N, Molnár Z. 2005. Functional thalamocortical synapse reorganization from subplate to layer IV during postnatal development in the reeler-like mutant rat (shaking rat Kawasaki). J Neurosci. 25:1395–1406.
Hur EE, Zaborszky L. 2005. Vglut2 afferents to the medial prefrontal and primary somatosensory cortices: a combined retrograde tracing in situ hybridization. J Comp Neurol. 483:351–373.
Ichinohe N, Rockland KS. 2004. Region specific micromodularity in the uppermost layers in primate cerebral cortex. Cereb Cortex. 14:1173–1184.
Ichinohe N, Yoshihara Y, Hashikawa T, Rockland KS. 2003. Developmental study of dendritic bundles in layer 1 of the rat granular retrosplenial cortex with special reference to a cell adhesion molecule, OCAM. Eur J Neurosci. 18:1764–1774.
Janusonis S, Gluncic V, Rakic P. 2004. Early serotonergic projections to Cajal-Retizus cells: relevance for cortical development. J Neurosci. 24:1652–1659.
Jensen KF, Killackey HP. 1987. Terminal arbors of axons projecting to the somatosensory cortex of the adult rat. II. The altered morphology of thalamocortical afferents following neonatal infraorbital nerve cut. J Neurosci. 7:3544–3553.
Jones EG. 1985. The thalamus. New York: Plenum.
Jones EG. 2001. The thalamic matrix and thalamocortical synchrony. Trends Neurosci. 24:595–601.
Jones EG, Hendry SH. 1989. Differential calcium binding protein immunoreactivity distinguishes classes of relay neurons in monkey thalamic nuclei. Eur J Neurosci. 1:222–246.
Kageyama GH, Robertson RT. 1993. Development of geniculocortical projections to visual cortex in rat: evidence early ingrowth and synaptogenesis. J Comp Neurol. 335:123–148.
Kato N. 1987. The postnatal development of thalamocortical projections from the pulvinar in the cat. Exp Brain Res. 68:533–540.
Kato N, Kawaguchi S, Miyata H. 1986. Postnatal development of afferent projections to the lateral suprasylvian visual area in the cat: an HRP study. J Comp Neurol. 252:543–554.
Kato N, Kawaguchi S, Yamamoto T, Samejima A, Miyata H. 1983. Postnatal development of the geniculocortical projection in the cat: electrophysiological and morphological studies. Exp Brain Res. 51:65–72.
Kawaguchi S, Samejima A, Yamamoto T. 1983. Post-natal development of the cerebello-cerebral projection in kittens. J Physiol (Lond). 343:215–232.
Krug K, Smith AL, Thompson ID. 1998. The development of topography in the hamster geniculo-cortical projection. J Neurosci. 18: 5766–5776.
Larkum ME, Senn W, Luscher HR. 2004. Top-down dendritic input increases the gain of layer 5 pyramidal neurons. Cereb Cortex. 14:1059–1070.
Lin RC, Nicolelis MA, Zhou HL, Chapin JK. 1996. Calbindin-containing non-specific thalamocortical projecting neurons in the rat. Brain Res. 711:50–55.
Linke R. 1999. Organization of projections to temporal cortex originating in the thalamic posterior intralaminar nucleus of the rat. Exp Brain Res. 127:314–320.
Llinás RR, Leznik E, Urbano FJ. 2002. Temporal binding via cortical coincidence detection of specific and nonspecific thalamocortical inputs: a voltage-dependent dye-imaging study in mouse brain slices. Proc Natl Acad Sci USA. 99: 449–454.
Lopez-Bendito G, Cautinat A, Sanchez JA, Bielle F, Flames N, Garratt AN, Talmage DA, Role LW, Charnay P, Marin O, et al. 2006. Tangential neuronal migration controls axon guidance: a role for neuregulin-1 in thalamocortical axon navigation. Cell. 125:127–142.
López-Bendito G, Molnár Z. 2003. Thalamocortical development: how are we going to get there? Nat Rev Neurosci. 4:276–289.
Lorente de No R. 1938. Cerebral Cortex: architecture, intracortical connections, motor projections. In: Fulton J, editor. Physiology of the nervous system. London: Oxford University Press. p. 291–340.
Lu SM, Lin RC. 1993. Thalamic afferents of the rat barrel cortex: a light- and electron-microscopic study using Phaseolus vulgaris leucoagglutinin as an anterograde tracer. Somatosens Mot Res. 10:1–16.
Lund RD, Mustari MJ. 1977. Development of the geniculocortical pathway in rats. J Comp Neurol. 173:289–305.
Macchi G, Bentivoglio M, Minciacchi D, Molinari M. 1996. Trends in the anatomical organization and functional significance of the mammalian thalamus. Ital J Neurol Sci. 17:105–129.
Mann F, Zhukareva V, Pimenta A, Levitt P, Bolz J. 1998. Membrane-associated molecules guide limbic and nonlimbic thalamocortical projections. J Neurosci. 18:9409–9419.
Mann F, Peuckert C, Dehner F, Zhou Z, Bolz J. 2002. Ephrins regulate the formation of terminal axonal arbors during the development of thalamocortical projections. Development. 129:3945–3955.
Marotte LR, Leamey CA, Waite PM. 1997. Timecourse of development of the wallaby trigeminal pathway: III. Thalamocortical and corticothalamic projections. J Comp Neurol. 387:194–214.
Metin C, Godement P. 1996. The ganglionic eminence may be an intermediate target for corticofugal and thalamocortical axo. J Neurosci. 16:3219–3235.
McQuillen PS, DeFreitas MF, Zada G, Shatz CJ. 2002. A novel role for p75NTR in subplate growth cone complexity and visual thalamocortical innervation. J Neurosci. 22:3580–3593.
Meyer G, Soria JM, Martinez-Galán JR, Martin-Clemente B, Fairén A. 1998. Different origins and developmental histories of transient neurons in the marginal zone of the fetal and neonatal rat cortex. J Comp Neurol. 397:493–518.

Miller B, Chou L, Finlay, BL. 1993. The early development of thalamocortical and corticothalamic projections J Comp Neurol. 335:16–41.
Mitchell BD, Cauller LJ. 2001. Corticocortical and thalamocortical projections to layer I of the frontal neocortex in rats. Brain Res. 921:68–77.
Molnár Z, Adams R, Blakemore C. 1998. Mechanisms underlying the establishment of topographically ordered early thalamocortical connections in the rat. J Neurosci. 18:5723–5745.
Molnár Z, Blakemore C. 1999. Development of signals influencing the growth and termination of thalamocortical axons in organotypic culture. Exp Neurol. 156:363–393.
Molnar Z, Cordery P. 1999. Connections between cells of the internal capsule, thalamus and cerebral cortex in the embryonic rat. J Comp Neurol. 413:1–25.
Monconduit L, Villanueva L. 2005. The lateral ventromedial thalamic nucleus spreads nociceptive signals from the whole body surface to layer I of the frontal cortex. Eur J Neurosci. 21:3395–3402.
Naegele JR, Jhaveri S, Schneider GE. 1988. Sharpening of topographical projections and maturation of geniculocortical axon arbors in the hamster. J Comp Neurol. 277:593–607.
Noctor SC, Palmer SL, McLaughlin DF, Juliano SL. 2001. Disruption of layers 3 and 4 during development results in altered thalamocortical projections in ferret somatosensory cortex. J Neurosci. 21:3184–3195.
O'Leary DD, Terashima T. 1988. Cortical axons branch to multiple subcortical targets by interstitial axon budding: implications for target recognition and "waiting periods". Neuron. 1:901–910.
Parnavelas JG, Chatzissavidou A. 1981. The development of the thalamic projections to layer I of the visual cortex of the rat. Anat Embryol (Berl). 163:71–75.
Parnavelas JG, Chatzissavidou A, Burne RA. 1981. Subcortical projections to layer I of the visual cortex, area 17, of the rat. Exp Brain Res. 41:184–187.
Paxinos G, Watson C. 1998. The rat brain in stereotaxic coordinates. 4th ed. San Diego: Academic Press.
Penny GR, Itoh K, Diamond IT. 1982. Cells of different sizes in the ventral nuclei project to different layers of the somatic cortex in the cat. Brain Res. 242:55–65.
Portera-Cailliau C, Weimer RM, De Paola V, Caroni P, Svoboda K. 2005. Diverse modes of axon elaboration in the developing neocortex. PLoS Biol. 3:e272.
Poskanzer K, Needleman LA, Bozdagi O, Huntley GW. 2003. N-cadherin regulates ingrowth and laminar targeting of thalamocortical axons. J Neurosci. 23:2294–2305.
Price DJ, Kennedy H, Dehay C, Zhou L, Mercier M, Jossin Y, Goffinet AM, Tissir F, Blakey D, Molnar Z. 2006. The development of cortical connections. Eur J Neurosci. 23:910–920.
Rakic P. 1977. Prenatal development of the visual system in the rhesus monkey. Philos Trans R Soc Lond B Biol Sci. 278:245–260.
Rausell E, Avendaño C. 1985. Thalamocortical neurons projecting to superficial and to deep layers in parietal, frontal and prefrontal regions in the cat. Brain Res. 347:159–165.
Rausell E, Bickford L, Manger PR, Woods TM, Jones EG. 1998. Extensive divergence and convergence in the thalamocortical projection to the monkey somatosensory cortex. J Neurosci. 18:4216–4232.
Rausell E, Jones EG. 1991. Chemically distinct compartments of the thalamic VPM nucleus in monkeys relay principal and spinal trigeminal pathways to different layers of the somatosensory cortex. J Neurosci. 11:226–237.
Rieck RW, Carey RG. 1985. Organization of the rostral thalamus in the rat: evidence for connections to layer I of visual cortex. J Comp Neurol. 234:137–154.
Rubio-Garrido P, Pérez-de-Manzo F, Clascá F. 2004. Thalamic input to neocortical layer I in the rat: mapping of its sources and evidence for a highly converging system. FENS Abstr. 2:A224.10.
Seibt J, Schuurmans C, Gradwhol G, Dehay C, Vanderhaeghen P, Guillemot F, Polleux F. 2003. Neurogenin2 specifies the connectivity of thalamic neurons by controlling axon responsiveness to intermediate target cues. Neuron. 39:439–452.
Senft SL, Woolsey TA. 1991. Growth of thalamic afferents into mouse barrel cortex. Cereb Cortex. 1:308–335.
Shatz CJ, Luskin MB. 1986. Relationship between the geniculocortical afferents and their cortical target cells during development of the cat's primary visual cortex. J Neurosci. 6:3655–3668.
Sheng XM, Marotte LR, Mark RF. 1991. Development of the laminar distribution of thalamocortical axons and corticothalamic cell bodies in the visual cortex of the wallaby. J Comp Neurol. 307: 17–38.
Shimogori T, Grove EA. 2005. Fibroblast growth factor 8 regulates neocortical guidance of area-specific thalamic innervation. J Neurosci. 25:6550–6560.
Shlosberg D, Amitai Y, Azouz R. 2006. Time-dependent, layer-specific modulation of sensory responses mediated by neocortical layer 1. J Neurophysiol. 96:3170–3182.
Skaliora I, Adams R, Blakemore C. 2000. Morphology and growth patterns of developing thalamocortical axons. J Neurosci. 20:3650–3662.
Soussi-Yanicostas N, de Castro F, Julliard AK, Perfettini I, Chedotal A, Petit C. 2002. Anosmin-1, defective in the X-linked form of Kallmann syndrome, promotes axonal branch formation from olfactory bulb output neurons. Cell. 109:217–228.
Sur M, Esguerra M, Garraghty PE, Kritzer MF, Sherman SM. 1987. Morphology of physiologically identified retinogeniculate X- and Y-axons in the cat. J Neurophysiol. 58:1–32.
Sur M, Rubenstein JL. 2005. Patterning and plasticity of the cerebral cortex. Science. 310:805–810.
Szebenyi G, Callaway JL, Dent EW, Kalil K. 1998. Interstitial branches develop from active regions of the axon demarcated by the primary growth cone during pausing behaviors. J Neurosci. 18:7930–7940.
Szebenyi G, Dent EW, Callaway JL, Seys C, Lueth H, Kalil K. 2001. Fibroblast growth factor-2 promotes axon branching of cortical neurons by influencing morphology and behavior of the primary growth cone. J Neurosci. 21:3932–3941.
Tang F, Kalil K. 2005. Netrin-1 induces axon branching in developing cortical neurons by frequency-dependent calcium signaling pathways. J Neurosci. 25:6702–6715.
Thomson AM, Bannister AP. 2003. Interlaminar connections in the neocortex. Cereb Cortex. 13:5–14.
Uziel D, Muhlfriedel S, Zarbalis K, Wurst W, Levitt P, Bolz J. 2002. Miswiring of limbic thalamocortical projections in the absence of ephrin-A5. J Neurosci. 22:9352–9357.
Vanderhaeghen P, Polleux F. 2004. Developmental mechanisms patterning thalamocortical projections: intrinsic, extrinsic and in between. Trends Neurosci. 27:384–391.
Vogt BA. 1991. The role of layer I in cortical function. In: Peters A, Jones EG, editors. Cerebral cortex. Vol. 9. New York: Plenum Press. p. 49–80.
Wang Y, Kurata K. 1998. Quantitative analyses of thalamic and cortical origins of neurons projecting to the rostral and caudal forelimb motor areas in the cerebral cortex of rats. Brain Res. 781: 135–147.
White EL, Keller A. 1989. Cortical circuits: synaptic organization of the cerebral cortex: structure, function, and theory. Boston: Birkhäuser.
Wise SP, Jones EG. 1977. Developmental studies of thalamocortical and commissural connections in the rat somatic sensory cortex. J Comp Neurol. 178:187–208.
Yamamoto N, Hanamura K. 2005. Formation of the thalamocortical projection regulated differentially by BDNF- and NT-3-mediated signaling. Rev Neurosci. 16:223–231.
Yamamoto N, Higashi S, Toyama K. 1997. Stop and branch behaviors of geniculocortical axons: a time-lapse study in organotypic cocultures. J Neurosci. 17:3653–3663.
Yamamoto N, Inui K, Matsuyama Y, Harada, A, Hanamura K, Murakami F, Ruthazer ES, Rutishauser U, Seki T. 2000. Inhibitory mechanism by polysialic acid for lamina-specific branch formation of thalamocortical axons. J Neurosci. 20:9145–9151.